An Assessment of Flooding and Drying Techniques for Use in the ADCIRC Hydrodynamic Model:

Implementation and Performance in One-Dimensional Flows

Richard A. Luettich, Jr.
University of North Carolina at Chapel Hill
Institute of Marine Sciences
3431 Arendell St.
Morehead City, NC 28557

Joannes J. Westerink
Dept. of Civil Engineering and Geological Sciences
University of Notre Dame
Notre Dame, IN 46556

January 30, 1995

Contractors Report

Prepared for the DEPARTMENT OF THE ARMY
Coastal Engineering Research Center
Waterways Experiment Station
US Army Corps of Engineers
Vicksburg, MS 39180

Under Contract No. DACW39-94-M-5869

TABLE OF CONTENTS

INTRODUCTION

The present implementation (version 26.XX) of the 2D/3D hydrodynamic model ADCIRC (Luettich et al, 1992, Westerink et al, 1994) makes no allowance for the flooding or drying of tidal flats during the course of a tidal cycle or for the inundation and recession of water from low lying coastal lands in response to coastal storms. Rather, ADCIRC assumes the land-water boundary is fixed regardless of the water surface elevation. To accommodate this assumption, (i) bathymetric water depths are artificially deepened near shore so that nodes never become dry during falling water levels and (ii) coastlines are assumed to represent infinitely high vertical walls which water piles up against during rising water levels. While these assumptions are reasonable for modeling large scale coastal flows, they improperly represent frictional dissipation and finite amplitude nonlinearities in near shore regions and they also prohibit the over land propagation of flood waters associated with storm surge. As a result, coastal storm surge elevations are often over-estimated and the extent of inundation, a critical parameter in the use of hydrodynamic models for coastal planning, can not accurately be assessed.

Prior to implementing any flooding and drying capability into ADCIRC, we have reviewed flooding and drying algorithms and capabilities as reported in the published literature. A summary of our findings is presented below. The remainder of this report describes our implementation, testing and assessment of several potential flooding and drying algorithms in a one-dimensional (vertically and laterally integrated, constant width) analogue of ADCIRC. The simplicity of the 1D code allowed a much more rapid and thorough assessment of these approaches than would have been possible using the full ADCIRC model. To this point we have concentrated on flooding and drying of sloping inclines rather than flow across intermittently submerged barriers. Provided the flow across a barrier is assumed to exit the computational domain, this feature can be implemented in ADCIRC in a straight forward manner as a discharge boundary condition with the discharge rate determined using an appropriate weir formula.

LITERATURE SURVEY

The inclusion of flooding and drying capabilities in a hydrodynamic model is a difficult problem. Past attempts to deal with these processes can be broadly lumped into two categories, spatially deforming computational grid schemes and spatially fixed computational grid schemes.

The use of spatially deforming grids requires the transformation of the governing equations into a horizontal coordinate system that is advected with the mean flow. For every time step the water level, the horizontal velocity and the position of the grid is recomputed. Although this approach is conceptually attractive, in practice it can lead to highly deformed grids and is typified by high computational costs. Consequently, it has primarily been restricted to applications involving idealized test problems, (Sielecki and

Wurtele, 1970; Lynch and Gray, 1980; Johns 1982; Akanbi and Katopodes, 1988; Siden and Lynch, 1988; Austria and Aldama, 1990).

The most common approach to flooding and drying in operational hydrodynamic models assumes the computational grid is fixed in space. At the beginning of the model simulation each cell (for a finite difference model) or element (for a finite element model) is designated as being either "wet" or "dry". Wet areas participate in the hydrodynamic calculations while dry areas do not. At designated times (which may or may not be every model time step) an assessment is made of whether additional areas in the grid have become wet or dry and therefore whether they will participate in the next model computation. Since the grid is fixed in space, areas are restricted to wetting or drying in whole grid increments. Examples of this type of wetting and drying strategy can be found in Reid and Bodine (1968), Flather and Heaps (1975), Yeh and Chou (1979), Hubbert and Flather (1987), Leendertse (1987), Yu et al. (1990), Cialone (1991), and Jelesnianski et al. (1992). We note that the specific implementation details of the wetting and drying algorithms in fixed grid models vary from model to model. For example WIFM assumes cells wet and dry according to a broad crested weir formula, (Cialone, 1991). Other models use the long wave equations (often without the advective terms included) to wet and dry cells, (Reid and Bodine, 1968; Leendertse, 1987; Jelesnianski et al., 1992). Also, most operational models allow for the possibility of sub grid scale barriers by using weir formulae in place of or in combination with the long wave equations when these features are encountered. A consistent problem with the fixed grid approaches is numerical noise generated when grid cells are turned on and off. Bottom friction is fairly effective at damping this noise in shallow water, although other strategies (such as limiting the frequency at which cells can wet and dry) have been used to control more persistent noise problems.

Our search of the literature of existing flooding and drying algorithms suggests that deforming grid schemes offer a methodology that closely adheres to the long wave equations. However, their significant computational expense makes them presently impractical for use in an operational model. Fixed grid schemes, despite their often ad hoc nature, have been implemented in operational models and demonstrated to give realistic flooding and drying estimates. Therefore, we have initially chosen to explore implementing a spatially fixed computational grid scheme in ADCIRC.

SUMMARY OF POTENTIAL FIXED GRID FLOODING AND DRYING ALGORITHMS

We have implemented and tested three spatially fixed computational grid algorithms for possible inclusion into ADCIRC. The rationale and implementation of these are discussed below.

Pure Drag Coefficient Approach (DCA)

The DCA assumes that the drag coefficient can be set high enough at "dry" nodes that it will effectively prevent water from moving at those nodes. Therefore, *both wet and dry nodes* participate equally in the model computations.

The implementation of the DCA is quite easy. To cold start the model, the water level departure from the geoid, ζ, is defined as zero for all "wet" nodes (bathymetric depths below the geoid) and as $|h| + H_{\min}$, where $H_{\min}$ is a minimum depth, (on the order of 1 cm), for all "dry" nodes (bathymetric depths above the geoid). All model computations proceed essentially as they are presently implemented in ADCIRC. The only difference is that a new value of the drag coefficient must be computed throughout the model domain every time step, depending on the water depth. At present we simply multiply the deep water drag coefficient, $C_{f\min}$, by a large number (e.g., 100 - 1000) when $H < 2H_{\min}$. Also, if the water depth drops below $H_{\min}$ due to leakage at dry nodes, it is set back to $H_{\min}$. A particular attraction of the DCA is that the GWCE system matrix remains stationary in time and therefore needs only to be set up and decomposed once during the model simulation. This provides significant computational savings when the direct matrix solver is used with a nonlumped, implicit, GWCE formulation.

Our experience with the DCA in 1D has identified two difficulties with this approach. (i) It is difficult to specify a drag coefficient that effectively freezes water motion at dry nodes without causing the model to become unstable. Consequently, we must continually raise the water depths at "dry" nodes back up to $H_{\min}$, thereby adding mass to the system. In the test problems presented below, this has not appeared to have any noticeable impact on the solutions. (ii) Elements connected to both wet and dry nodes may have an undesirable behavior due to the fact that the water surface slope is effectively constrained at the dry node and free to move at the wet node. For example, consider water moving up a sloping incline. After a node first "wets" its water level may still be below that at the adjacent upslope dry node. The resulting water level gradient between these two nodes will create a physically unrealistic force that is adverse to the direction of water advancement and that may cause water to temporarily flow downslope (or "backwash") at the newly wetted node.

Nodal Wetting Approach (NWA)

The NWA assumes that flooding and drying can be represented by turning areas of the grid on and off on a node by node basis. Conceptually, in 1D, this like raising and lowering one end of a row of dominoes that are laid flat and connected end to end using hinges. We note that the NWA is physically quite similar to the DCA, except that the NWA formally turns nodes off that have become dry while the DCA relies on high friction to effectively turn the nodes off.

The implementation of this approach is not quite as easy as the DCA. To cold start the model, ζ is defined as zero for all "wet" nodes and as $|h| + H_{\min}$ for all "dry" nodes. At subsequent time steps wet node computations proceed as they are presently implemented in ADCIRC. However, at all dry nodes, ζ^{k+1} (where k+1 denotes the time

level presently being solved for) is fixed at its value at time level k by placing a 1 on the diagonal of the GWCE system matrix and by setting the right hand side equal to ζ^k. After solving the GWCE equation for ζ, the water depth is checked at each node in the grid. If a node is currently classified as wet and the water depth drops below the minimum depth, the node is considered to have dried. If a node is currently dry and ζ at any adjacent wet node rises above ζ at the node being checked, the node is considered to have wetted. The velocity is zeroed out at dry nodes.

The implementation of the NWA in ADCIRC is somewhat unattractive because the system matrix in the GWCE must be modified each time a node changes its status from wet or dry. When this happens, the banded GWCE matrix must be re-decomposed if the direct matrix solver is used with a nonlumped, implicit formulation of the GWCE. This disadvantage is removed, however, if the iterative solver (e.g., preconditioned conjugate gradient solver) is used or a lumped, explicit form of the GWCE is solved.

Our experience with the NWA in 1D has identified two difficulties with this approach. (i) Mild shocks are introduced into the computations when nodes are turned on and off. (ii) Elements connected to both wet and dry nodes have the same undesirable behavior as described for the DCA. In practice, bottom friction helps to damp out numerical noise associated with the shocks and reduce physically unrealistic "backwash".

Elemental Wetting Approach (EWA)

The EWA assumes that flooding and drying can be represented by turning areas of the grid on and off on an element by element basis. Conceptually, this approach is similar to most of the previously employed fixed grid flooding and drying schemes that have been applied in finite difference codes. In 1D, the EWA assumes a slope is divided up by a series of removable, vertical barriers, (one barrier is located at each finite element node). The height of each barrier is equal to the ground elevation of the next node up the slope plus the minimum allowed water depth. All barriers whose tops lie below the still water level are removed. If the water level recedes, it moves down the face of a barrier until it hits the toe of the barrier plus the minimum depth. At that time the barrier at the next node down the slope is put in place thereby trapping all water up stream of it and causing the element to "dry". As the water level recedes further, it moves down the face of the newly placed barrier. If the water level rises, it moves upward along the face of a barrier until it reaches the top. When the top is reached the barrier is removed and the next element upstream "wets". As the water level rises further, it moves up the face of the barrier located at the next node up the slope. The result of this approach is a stair step like series of pools of water, each having a level surface, in the area of the domain that is above the present water level.

The implementation of this approach is comparable to the NWA. To cold start the model, ζ is defined as zero for all "wet" nodes and as $|h| + H_{\min}$ for all "dry" nodes, similar to the NWA and DCA. At subsequent time steps, computations proceed as they are presently implemented in ADCIRC for all nodes connected to at least one wet element.

Vertical wall boundaries are assumed along the land-water interface which is located at nodes lying between adjacent wet and dry elements. At all nodes surrounded by dry elements, ζ^{k+1} is fixed at its value at time level k as done in the NWA. After solving the GWCE equation for ζ, the water depth is checked at each node in the grid. If the water depth drops below the minimum depth at an active node, all elements containing this node are considered to have dried. If ζ at a node located on the land-water interface rises above ζ at the adjacent dry node, the connecting element is considered to have wetted. New land-water boundary nodes are then identified. Velocities are calculated as presently implemented in ADCIRC for all nodes connected to wet elements. The velocity is zeroed out at all nodes that are surrounded by dry elements.

The implementation of the EWA in ADCIRC has the same disadvantage as the NWA; the system matrix in the GWCE must be modified each time an element changes its status from wet or dry. This means that the banded GWCE matrix must be re-decomposed each time any node changes status if the direct matrix solver is used with a nonlumped, implicit formulation of the GWCE. This disadvantage is removed, however, if the iterative solver is used or a lumped, explicit form of the GWCE is solved.

The primary difficulty we have experienced with the EWA in 1D is that rather strong shocks are introduced into the computations when elements turn on and off. Since the water level transitions are fairly smooth, these shocks must originate from the sudden change in velocity when a barrier is introduced or removed. However, as found for the NWA, bottom friction is fairly effective at damping out numerical noise associated with the resulting shocks in 1D.

DEPTH DEPENDENT DRAG COEFFICIENT

To complement the flooding and drying schemes described above, we have designed a drag coefficient that is inversely proportional to water depth as:

$$C_f = C_{f\min}\left[1+\left(\frac{H_o}{H}\right)^{\theta}\right]^{\gamma/\theta} \tag{1}$$

where C_f is the standard 2D drag coefficient used in ADCIRC (applied using either a linear or quadratic friction relationship) and H is the total water depth. This relation has the behavior that C_f approaches $C_{f\min}$ in deep water, ($H > H_o$), and $C_{f\min}(H_o/H)^{\gamma}$ in shallow water, ($H < H_o$), Figure 1. The exponent θ determines how rapidly C_f approaches each asymptotic limit and γ determines how rapidly the friction coefficient increases as the water depth decreases. We note that if $C_{f\min} \equiv g n^2/H_o^{\gamma}$ and $\gamma = 1/3$, where g is the gravitational constant and n is the Manning coefficient, Eq. (1) will

provide a Manning equation type frictional behavior for $H < H_o$, Figure 1. Examples of the relationship between $C_{f\min}$ and n for $\gamma = 1/3$ are given in Table 1.

Table 1. Comparison between $C_{f\min}$ and n if $C_{f\min} = g n^2 / H_o^{1/3}$

$C_{f\min}$	n H_o=5m	n H_o=10m	n H_o=20m	n H_o=40m
0.0015	0.016	0.018	0.020	0.023
0.0020	0.019	0.021	0.024	0.026
0.0025	0.021	0.023	0.026	0.030
0.0030	0.023	0.025	0.029	0.032
0.0040	0.026	0.030	0.033	0.037
0.0050	0.030	0.033	0.037	0.042
0.0100	0.042	0.047	0.053	0.059

The DCA is the only flooding and drying scheme that specifically requires an elevated drag coefficient in shallow water (to keep water from running off "dry" areas). However, there is considerable observational evidence from fully turbulent open channel flows for the Manning drag law, (e.g., Chow 1959). Therefore it may be appropriate to use the Manning drag law in shallow coastal flows (whether or not flooding and drying occur). Eq. (1) allows the drag coefficient to remain constant at typical continental shelf water depths (as has been used in most previous ADCIRC simulations) and to adopt a Manning type behavior in shallow water.

We have used the Manning's equivalent to Eq. (1) in all flooding and drying test cases presented below.

TEST PROBLEMS

The three flooding and drying schemes outlined have been implemented in a one-dimensional (vertically and laterally integrated, constant width) analogue of ADCIRC. The test problems presented below are all designed to test tidally driven flooding and drying on sloping inclines. In all cases the model was run until a dynamic equilibrium was reached and the model results were stable from one tidal cycle to the next.

Flooding and Drying of a Frictionless Incline

One of the few flooding and drying problems for which an analytical solution can be found is the propagation of a long wave onto a sloping shore, Carrier and Greenspan (1958). This is a very difficult problem to solve numerically since without bottom friction there is little to damp noise generated in the solution. To our knowledge previous numerical solutions to this problem have all used deforming grid schemes (Sielecki and

Wurtele, 1970; Lynch and Gray, 1980; Johns 1982; Siden and Lynch, 1988), which appear to generate considerably less numerical noise than fixed grid schemes.

We were unable to obtain stable numerical solutions for this problem using the DCA or the EWA, with or with out the advective terms included in the computation, for any slopes of practical interest. However, we were able to obtain realistic, albeit somewhat noisy, numerical solutions for reasonable inclines using the NWA. Figures 2a-j compare analytical and numerical water levels and depth-averaged velocities every tenth of a tidal cycle in the downstream half of the domain for the following 1D channel:

channel length, 24km
bathymetric depth at open end, 5m below still water level
bathymetric depth at closed end, 1m above still water level
linear slope between open and closed end
numerical grid spacing, $\Delta x = 250m$
time step, $\Delta t = 30s$, $\left(\Delta t\sqrt{gh}/\Delta x\right)_{\max} = 0.85$
open end forcing 0.25m amplitude, 6h period.
$H_{\min} = 1$ cm
lumped, explicit GWCE formulation
no advective terms

Comparing Figures 2a and 2f indicates that the land-water boundary moves horizontally about 4.5 km and vertically about 1.2 m from high to low tide. The NWA water level solution is reasonably smooth and close to the analytical solution throughout the entire tidal cycle; the most significant errors occur near the front during rising water levels (Figures 2g-j). Away from the front the NWA velocity solution tracks the analytical solution reasonably well, although overall it is much noisier than the elevation solution and clearly suffers from the "backwash" problem near the front (Figures 2a-g). The strong downslope flows at the front as the tide moves from low slack water into the flooding cycle appear to introduce significant numerical instability into the velocity solution, Figures 2h-j. However, this quiets down by the time the tide reaches high slack water. We note that the solution is completely unstable if a consistent (as opposed to lumped) or partially implicit (as opposed to fully explicit) formulation was used for the GWCE or if the advective terms are included in the solution.

Flooding and Drying of a Frictional Incline, Case #1

This test case replicates the frictionless problem, except that realistic bottom friction has been added. The resulting problem may be typical of relatively weak forcing on a mild sloping shore (25cm/km). The specific problem parameters are:

channel length, 24km
bathymetric depth at open end, 5m below still water level
bathymetric depth at closed end, 1m above still water level
linear slope between open and closed end

numerical grid spacing, $\Delta x = 250m$
time step, $\Delta t = 30s$, $\left(\Delta t\sqrt{gh}/\Delta x\right)_{\max} = 0.85$
open end forcing 0.25m amplitude, 6h period.
$H_{\min} = 1$ cm
lumped, explicit GWCE formulation
advective terms included
$C_{f\min} = 0.0025, H_o = 1m, \theta = 10, \gamma = 1/3$
$C_f = 300\, C_{f\min}$ if $H < 2H_o$ in DCA

Water levels and depth-averaged velocities every tenth of a tidal cycle in the downstream half of the domain are presented in Figures 3a-j for model runs using the three flooding and drying algorithms. Due to the presence of friction, the excursion of the land-water boundary is smaller than in the previous test case. (In this problem the excursions are approximately 2km and 0.8m in the horizontal and vertical directions, respectively.) All three algorithms give very similar water level predictions throughout the domain. (Note, for the EWA, only the water level for the downstream element attached to each node has been plotted.) The largest differences occur in the velocity solutions near the front where the EWA solution is more damped than the DCA and NWA solutions. Despite these differences in the velocity solutions, the difference in flux is small due to the shallow water depths.

Beyond about 21.75km, the channel never floods and a steady downslope velocity of about 0.2 m/s develops for the DCA. This was the minimum amount of leakage we could enforce for this method since the code became unstable if a higher drag coefficient was used for the "dry" nodes. To balance this leakage it was necessary to continuously add water at the upstream end. The total volume of water (per unit width) added during a 6h tidal cycle was approximately $40m^2$. As expected, the NWA solution is quite similar to the DCA solution, except that the former is forced to have zero velocity on the permanently dry nodes

Flooding and Drying of a Frictional Incline, Case #2

This case demonstrates the algorithm behavior for a stronger forcing and steeper sloping shore (1m/km). The specific problem parameters are:

channel length, 24km
bathymetric depth 10m below still water level for first half of channel length
bathymetric depth at closed end, 2 m above still water level
linear slope between channel mid point and closed end
numerical grid spacing, $\Delta x = 250m$
time step, $\Delta t = 15s$, $\left(\Delta t\sqrt{gh}/\Delta x\right)_{\max} = 0.6$
open end forcing, 0.5m amplitude, 6h period.
$H_{\min} = 1$ cm
lumped, explicit GWCE formulation

advective terms included
$C_{f\min} = 0.0025, H_o = 1m, \theta = 10, \gamma = 1/3$
$C_f = 300\, C_{f\min}$ if $H < 2H_o$ in DCA

Water levels and depth-averaged velocities every tenth of a tidal cycle in the downstream third of the domain are presented in Figures 4a-j for model runs using the three flooding and drying algorithms. The higher forcing and steeper slope increase the vertical excursion of the land-water boundary to about 1.5m while limiting the horizontal excursion to approximately that of the previous test case. As in the previous case, all three algorithms give very similar water level predictions throughout the domain. (Note, for the EWA, only the water level for the downstream element attached to each node has been plotted.) The largest differences again occur in the velocity solutions near the front. The EWA solution is more damped at maximum ebb and near high and low slack than the other solutions, (Figures 4d,a,f, respectively). In general the EWA solution is also much smoother near the front than the others.

Beyond about 23km, the channel never floods and a steady downslope velocity of about 0.4 m/s develops for the DCA. This was the minimum amount of leakage we could enforce for this method since the code became unstable if a higher drag coefficient was used for the "dry" nodes. To balance this leakage it was necessary to continuously add water at the upstream end. The total volume of water (per unit width) added during a 6h tidal cycle was approximately $80m^2$. There is considerably more difference in the DCA and NWA velocity solutions in this test case, presumably due to different sources of numerical noise. In both solutions the "backwash" problem noted previously is clearly significant.

FLOODING AND DRYING IMPLEMENTATION IN TWO DIMENSIONS

The implementation of the DCA and the NWA in ADCIRC are essentially the same as in 1D. However, the implementation of the EWA is more difficult in ADCIRC than in 1D due to the need to correctly identify emerging, submerging and otherwise changing land-water boundaries in order to apply a normal flux boundary condition. – if used.
While this can be done, it will require considerably more effort than the other two algorithms given the present structure of the code and the need to maintain vectorization. Also, as noted previously, the NWA and EWA algorithms will require more computational effort to implement (due to the need to modify the GWCE system matrix) if a nonlumped or implicit model formulation is used together with the direct matrix solver. We also anticipate that the EWA may be noisier in 2D than it is in 1D. In 2D an element must wait to wet until the minimum depth at the highest node is surpassed by the water depths at both of the other nodes that make up the element. Since the required water level may not be reached simultaneously at both of the nodes, the water level discontinuity will be different at both nodes when the element wets.

SUMMARY AND CONCLUSIONS

Based on information available in the literature, we believe a fixed computational grid flooding and drying scheme would be most practical for short term implementation in the operational hydrodynamic model ADCIRC. Three fixed grid schemes have been implemented and tested to date in a 1D (vertically and laterally averaged, constant width) analogue of ADCIRC.

The drag coefficient approach (DCA) is by far the easiest to implement in 1D and 2D and imposes no direct penalties on the GWCE solution. The nodal wetting approach (NWA) is slightly more complicated to implement and requires the GWCE system matrix to be modified each time a node wets or dries. This carries with it a computational penalty when a direct matrix solver and an implicit, nonlumped GWCE formulation is used. The elemental wetting approach (EWA) is the most complicated to implement (due to the need to keep track of emerging, submerging and otherwise changing boundaries) and also requires the GWCE system matrix to be modified each time an element wets or dries.

The only analytical solution for a 1D flooding and drying problem that we are aware of is for the case of a frictionless channel with linearly sloping beach. Neither the DCA or EWA could handle this problem. However, the NWA gave encouraging elevation and reasonable, albeit noisy, velocity solutions. Further comparisons between the numerical algorithms on sloping beaches with friction showed that all three gave very similar water level responses. The EWA velocity solution was generally more damped and smoother than the other solutions. The DCA exhibited significant leakage velocities, although the accompanying mass flux was relatively small. Both the NWA and the DCA suffered from "backwash", particularly on the steeper beach. This is a likely contributor to the noise that characterized these solutions in the vicinity of the front.

As a complement to the flooding and drying algorithms, we have developed an empirical relationship that increase the drag coefficient as the water depth decreases in shallow water and holds the drag coefficient constant in deep water. The equation parameters can be conveniently set to obtain a Manning type friction behavior in shallow water. We anticipate using this relationship in ADCIRC in combination with a flooding and drying algorithm.

Based on its ease of implementation and the general agreement it gave in comparison with the other algorithms in the 1D test cases, we plan to initially implement the DCA flooding and drying scheme in ADCIRC. However, the seemingly superior performance of the EWA in our 1D test problems suggests that it might be desirable to implement this technique in ADCIRC at some point in the future.

Finally, we note that the following flooding and drying scheme that essentially combines the deforming and fixed grid approaches may merit consideration at some point in the future. In this "hybrid" scheme, a fixed grid would initially be laid out which contained wet and dry elements. Boundary elements (or perhaps several layers of

elements near the boundary) would be allowed to deform until an element adjacent to the boundary, (as laid out on the original fixed grid), was wholly engulfed. At that time the grid would be adjusted to include or exclude (depending on whether the water level was rising or falling) the engulfed element and the calculations continued. Using this approach water levels could be tracked in a more continuous manner than possible using a purely fixed grid approach, but at the same time near boundary element deformation would be limited and it would only be necessary to track the motion of nodes in a small fraction of the computational grid.

REFERENCES

Akanbi A.A., and N.D. Katopodes, 1988, "Model for Flood Propagation on Initially Dry Land", Journal of Hydraulic Engineering, **114**(7): 689-706.

Austria P.M. and A.A. Aldama, 1990, "Adaptive Mesh Scheme for Free Surface Flows with Moving Boundaries", In: Computational Methods in Surface Hydrology, G. Gambolati, A. Rinaldo, C. A. Brebbia, W. G. Gray and G. F. Pinder, eds., Springer-Verlag, pp 456-460.

Carrier, G.F. and H.P. Greenspan, 1958, "Water Waves of Finite Amplitude on a Sloping Beach", Journal of Fluid Mechanics, 4:97-109.

Chow, V.T., 1959, "Open Channel Hydraulics", McGraw-Hill, New York.

Cialone, J., 1991, "Coastal Modeling System (CMS) User's Manual", Instruction Report CERC-91-1, Coastal Engineering Research Center, U.S. Army Engineer Waterways Experiment Station, Vicksburg, MS.

Flather R.A. and N.S. Heaps, 1975, "Tidal Computations for Morecambe Bay", Geophysical Journal of Royal Astronomical Society, **42:**489-517.

Hubbert K.P. and R.A. Flather, 1987, "Tide and Surge Models for Shallow Water - Morcambe Bay Revisited", In Modeling Marine Systems, A.M. Davies, ed., pp 135-166.

Jelesnianski C.P., J. Chen and W.A. Shaffer, 1992, "SLOSH: Sea, Lake, and Overland Surges from Hurricanes", NOAA Technical Report NWS 48, 71p.

Johns B., 1982, "Numerical Integration of the Shallow Water Equations over a Sloping Shelf", International Journal for Numerical Methods in Fluids, **2:**253-261.

Leendertse J.J., 1987, "Aspects of SIMSYS2D, A System for Two-Dimensional Flow Computation", Rand Corportation report R-3572-USGS, p.

Luettich, R.A., Jr., J.J. Westerink and N.W. Scheffner, 1992, "ADCIRC: An Advanced Three-Dimensional Circulation Model for Shelves, Coasts and Estuaries; Report 1: Theory and Methodology of ADCIRC-2DDI and ADCIRC-3DL", Technical Report DRP-92-6, Coastal Engineering Research Center, U.S. Army Engineer Waterways Experiment Station, Vicksburg, MS.

Lynch D.R. and W.G. Gray, 1980, "Finite Element Simulation of Flow in Deforming Regions", Journal of Computational Physics, **36:**135-153.

Reid R.O. and B.R. Bodine, 1968, "Numerical Model for Storm Surges in Galveston Bay", Journal of the Waterways and Harbors Division, **94**(WW1):33-57.

Siden, G.L.D. and D.R. Lynch, 1988, "Wave Equation Hydrodynamics on Deforming Elements", International Journal for Numerical Methods in Fluids, **8:**1071-1093.

Sielecki A. and M.G. Wurtele, 1970, "The Numerical Integration of the Nonlinear Shallow-Water Equations with Sloping Boundaries", Journal of Computational Physics, **6:**219-236.

Westerink, J.J., Blain, C.A., R.A. Luettich, Jr., and N.W. Scheffner, 1994, "ADCIRC: An Advanced Three-Dimensional Circulation Model for Shelves, Coasts and Estuaries; Report 2: User's Manual for ADCIRC-2DDI", Technical Report DRP-92-6, Coastal Engineering Research Center, U.S. Army Engineer Waterways Experiment Station, Vicksburg, MS.

Yeh G. T. and F.K. Chou, 1979, "Moving Boundary Numerical Surge Model", Journal of the Waterway, Port, Coastal and Ocean Division, **105**(WW3):247-263.

Yu C.S., M. Fettweis, F. Rosswo and J. Berlamont, 1990, "A 2D Model with Changing Land-Water Boundaries", In: Computational Methods in Surface Hydrology, G. Gambolati, A. Rinaldo, C. A. Brebbia, W. G. Gray and G. F. Pinder, eds., Springer-Verlag, pp 101-106.

Figure 1. Comparison Between Manning Eqn. and Eqn. (1)

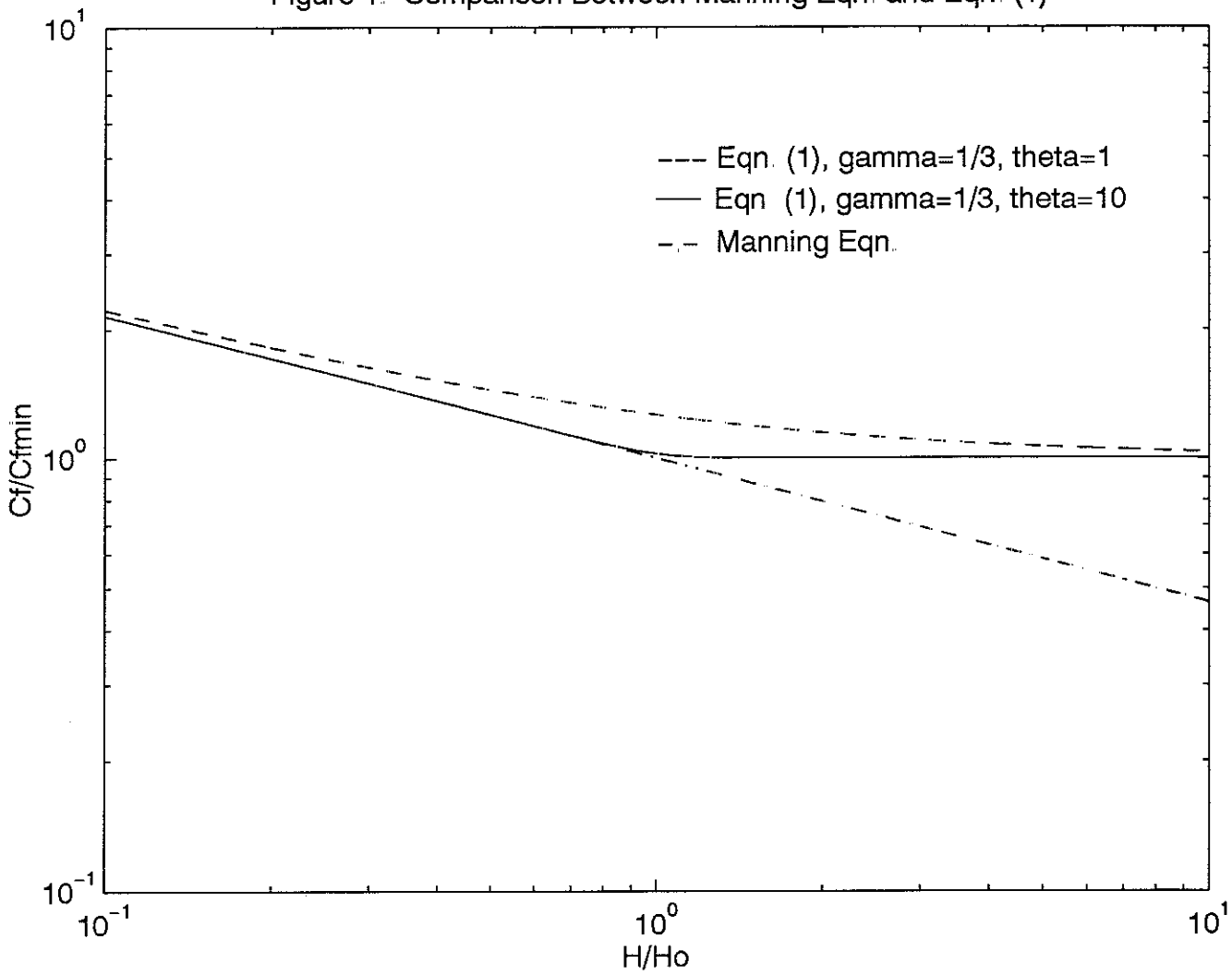

Figure 2a. Frictionless Test Case, Time = 0*T/10

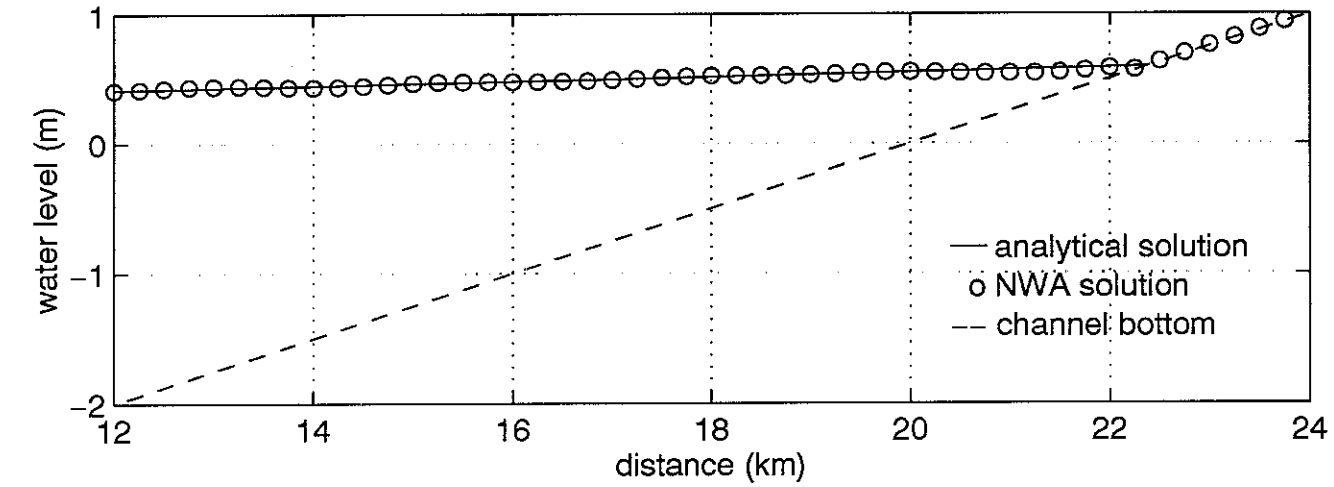

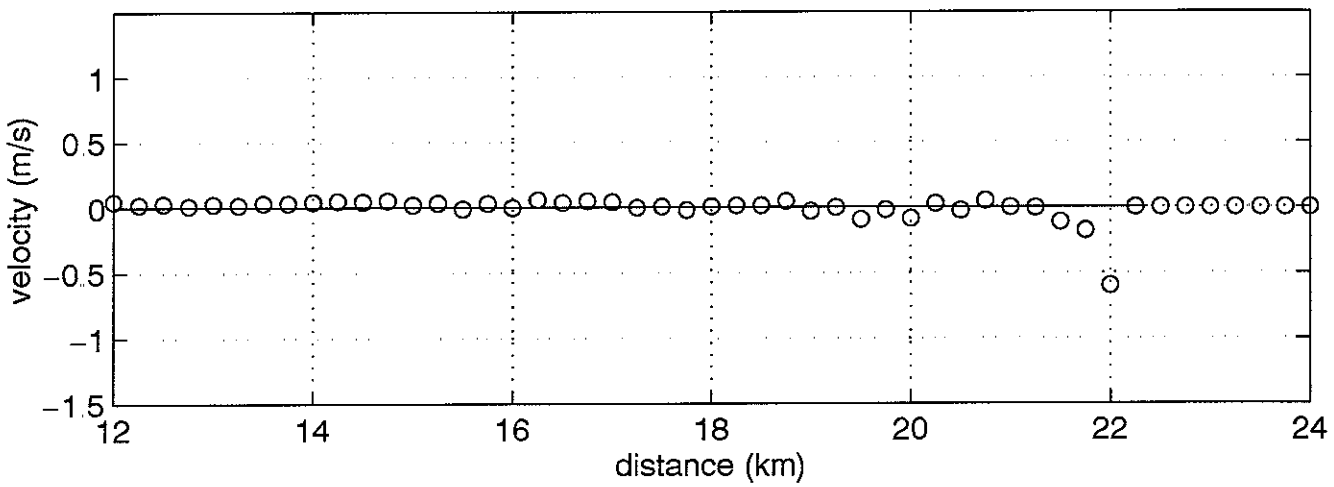

Figure 2b Frictionless Test Case, Time = 1*T/10

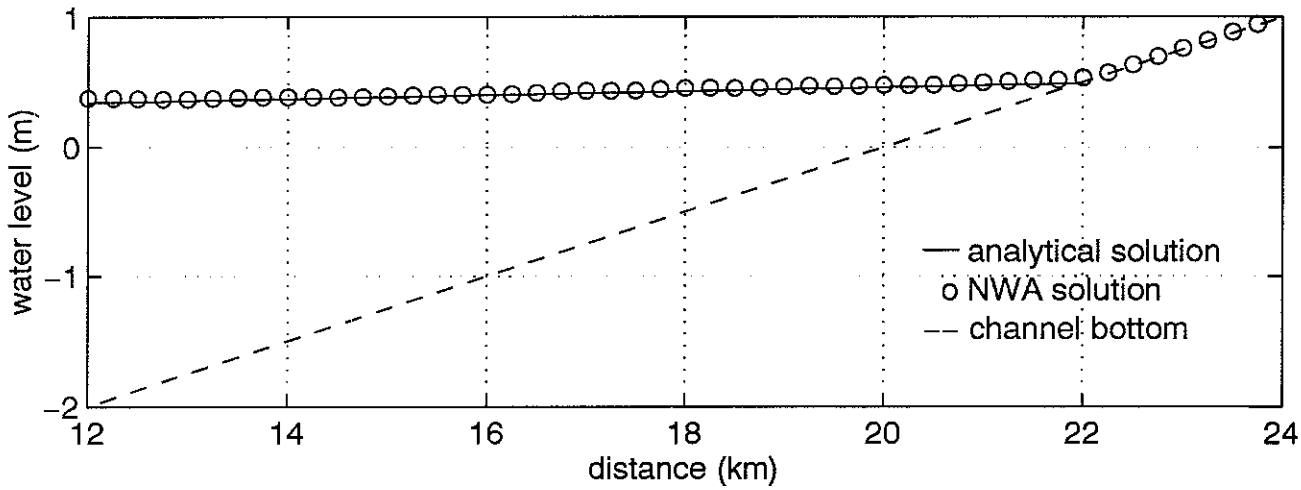

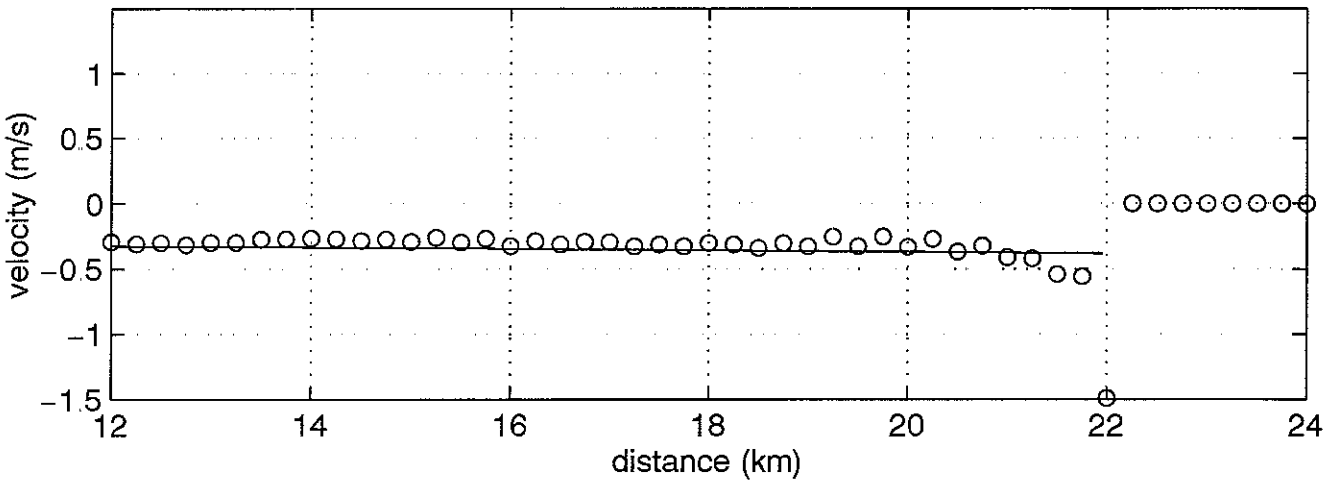

Figure 2c Frictionless Test Case, Time = 2*T/10

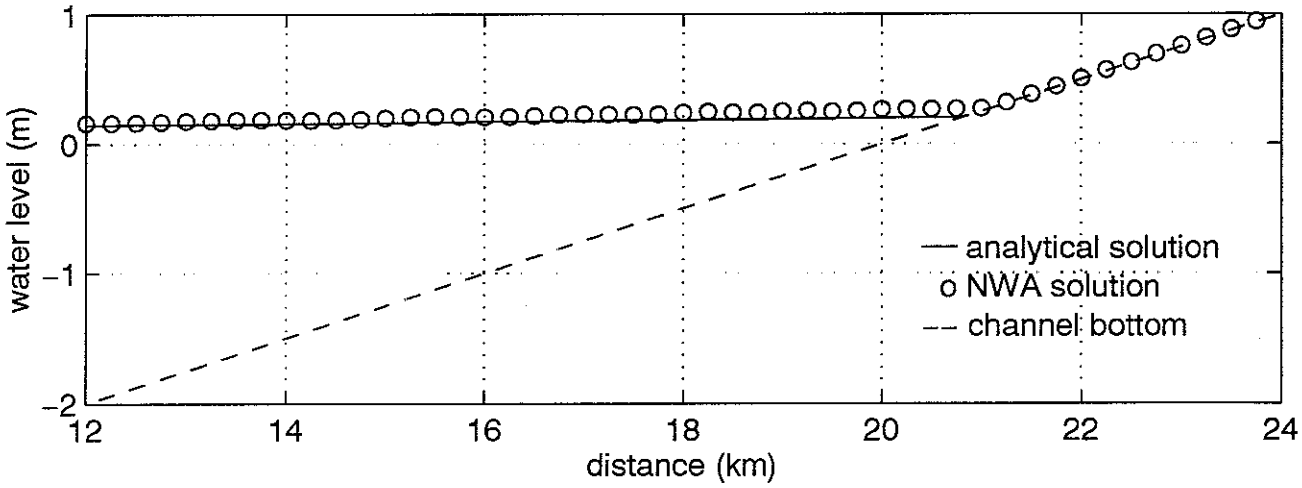

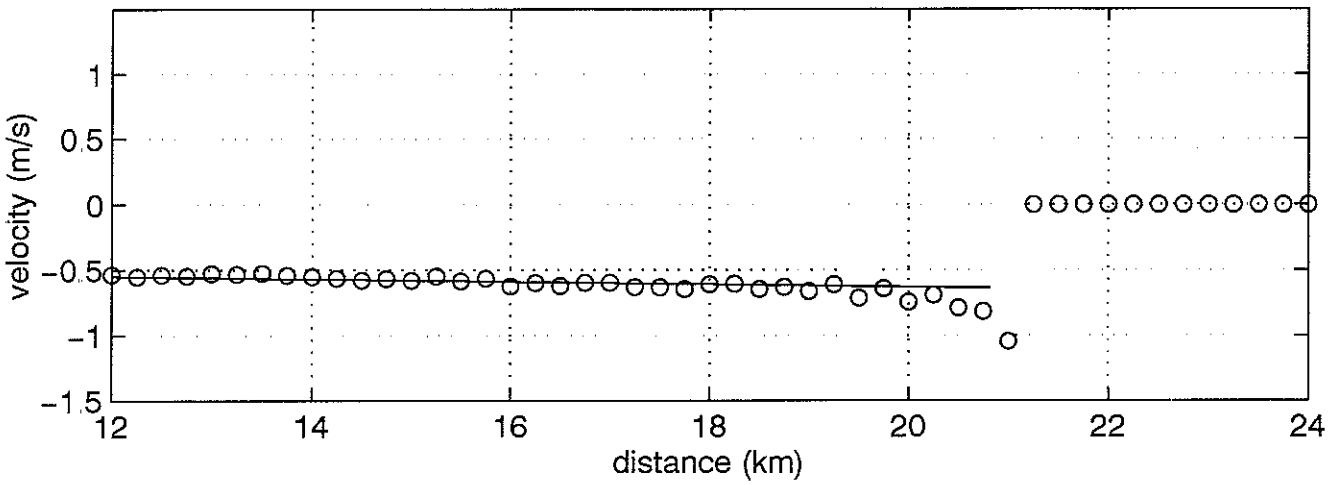

Figure 2d. Frictionless Test Case, Time = 3*T/10

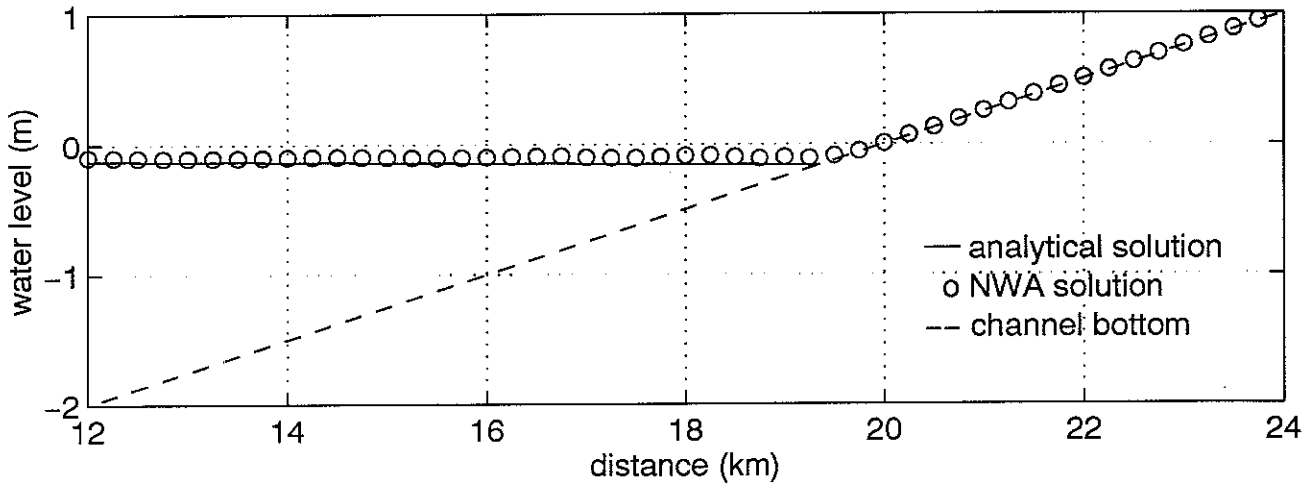

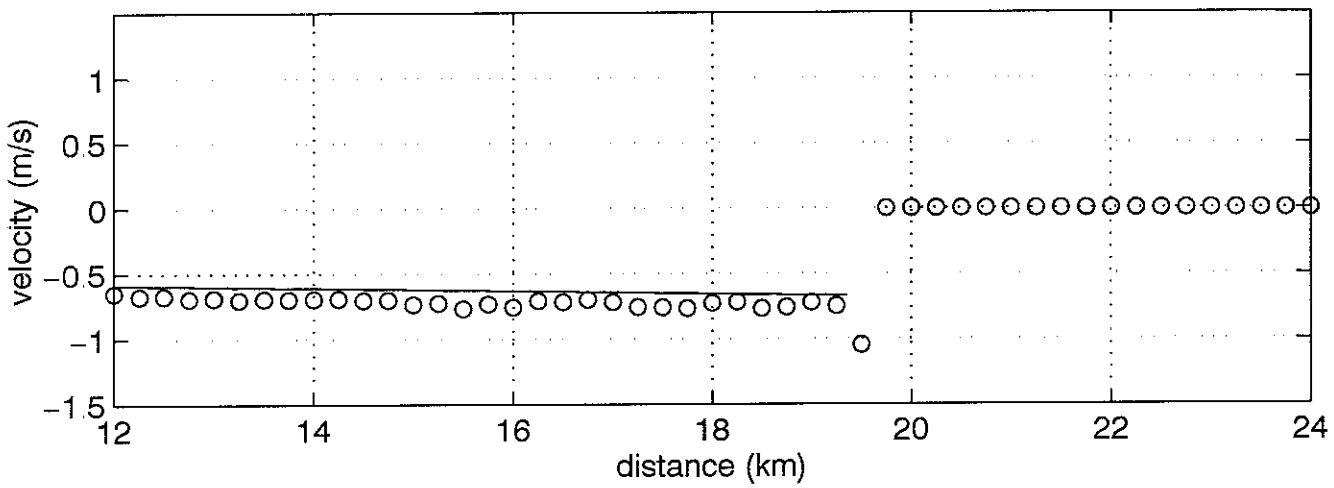

Figure 2e. Frictionless Test Case, Time = 4*T/10

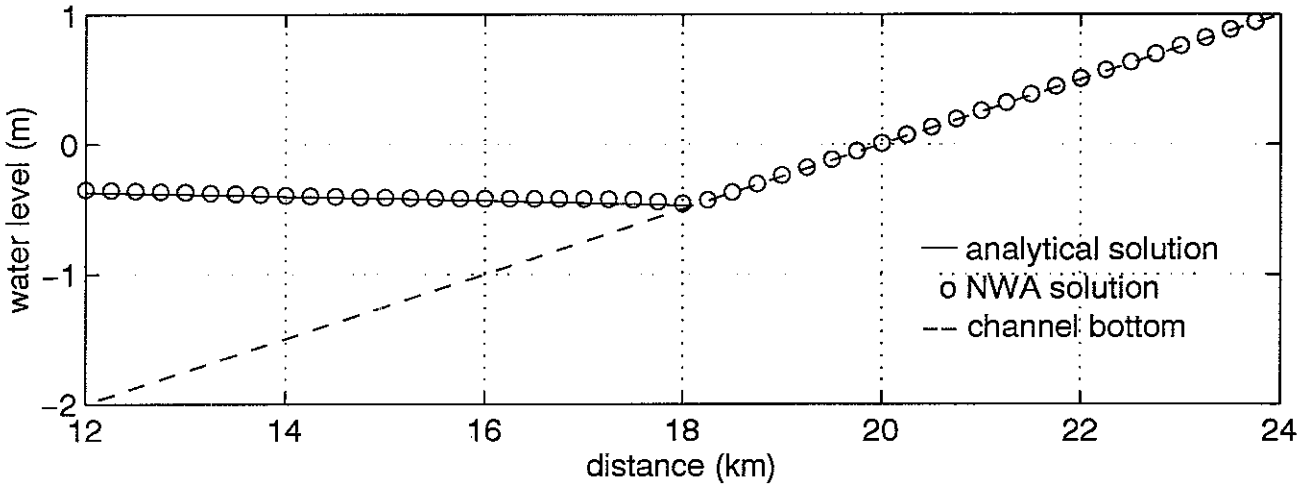

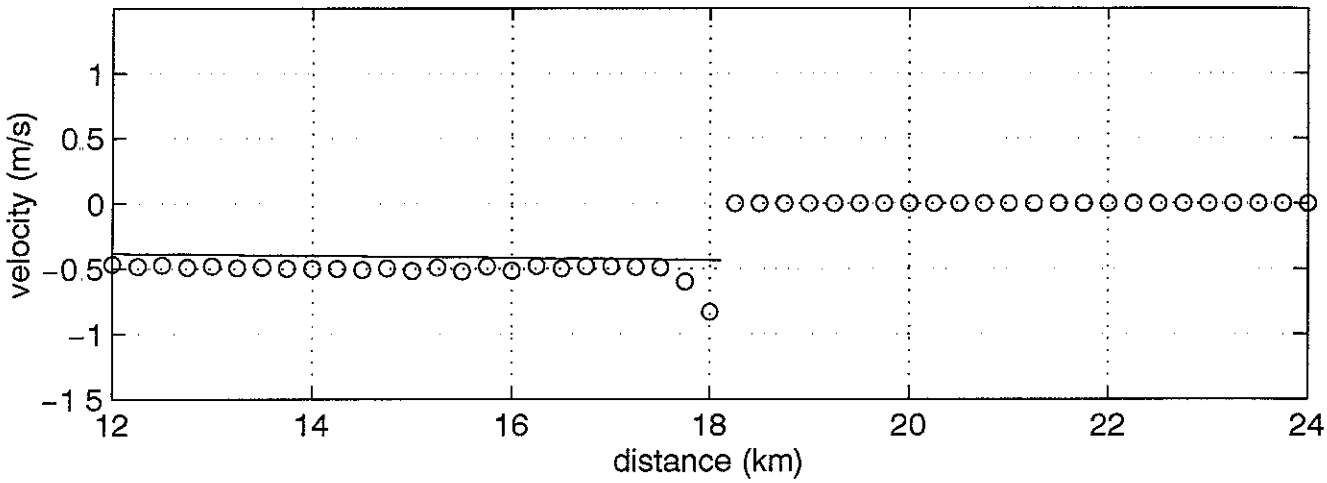

Figure 2f Frictionless Test Case, Time = 5*T/10

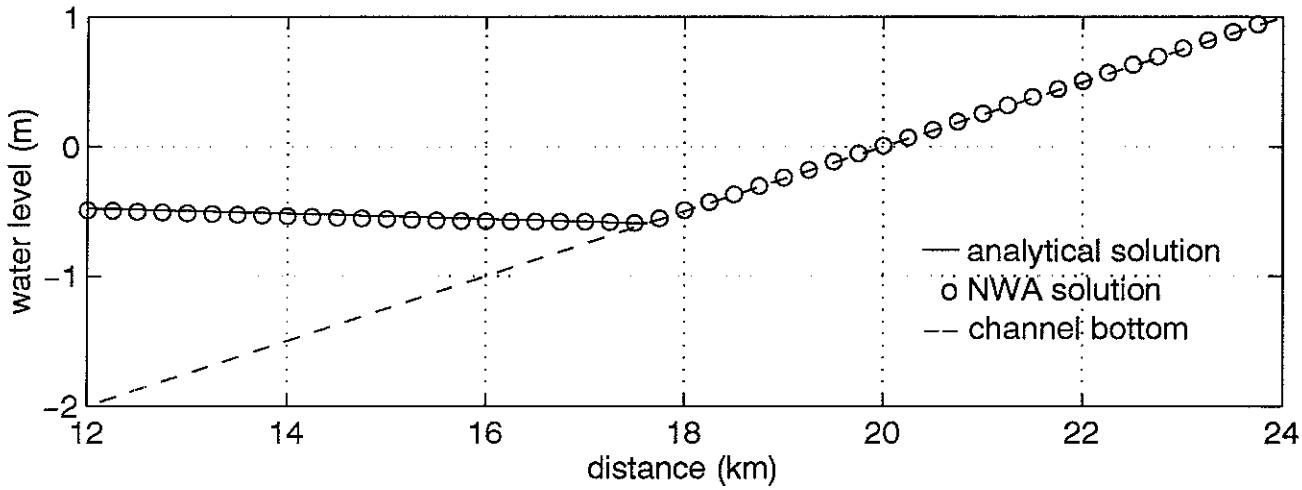

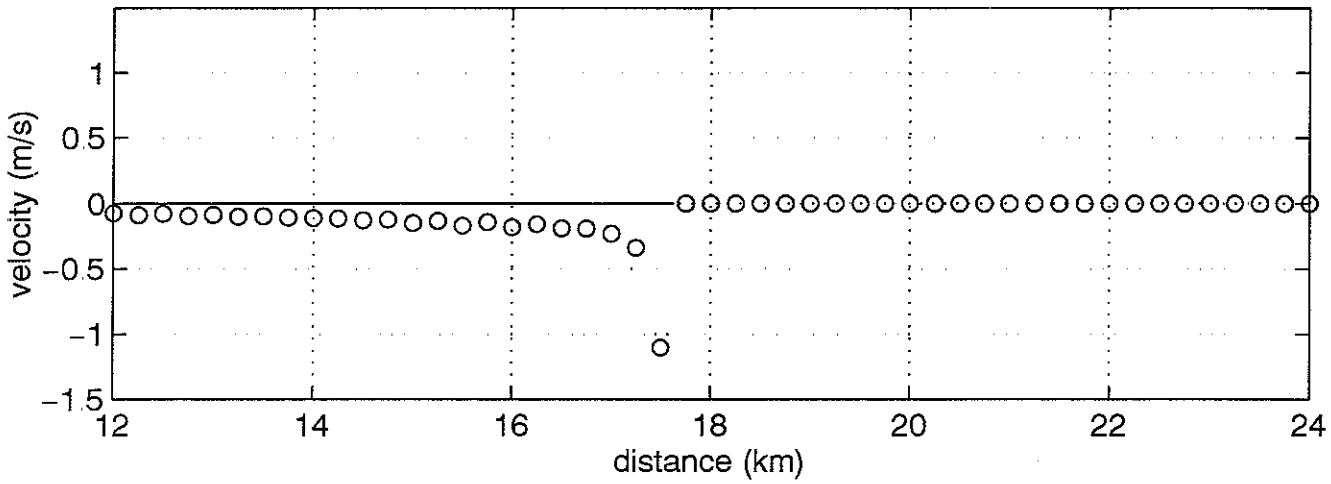

Figure 2g Frictionless Test Case, Time = 6*T/10

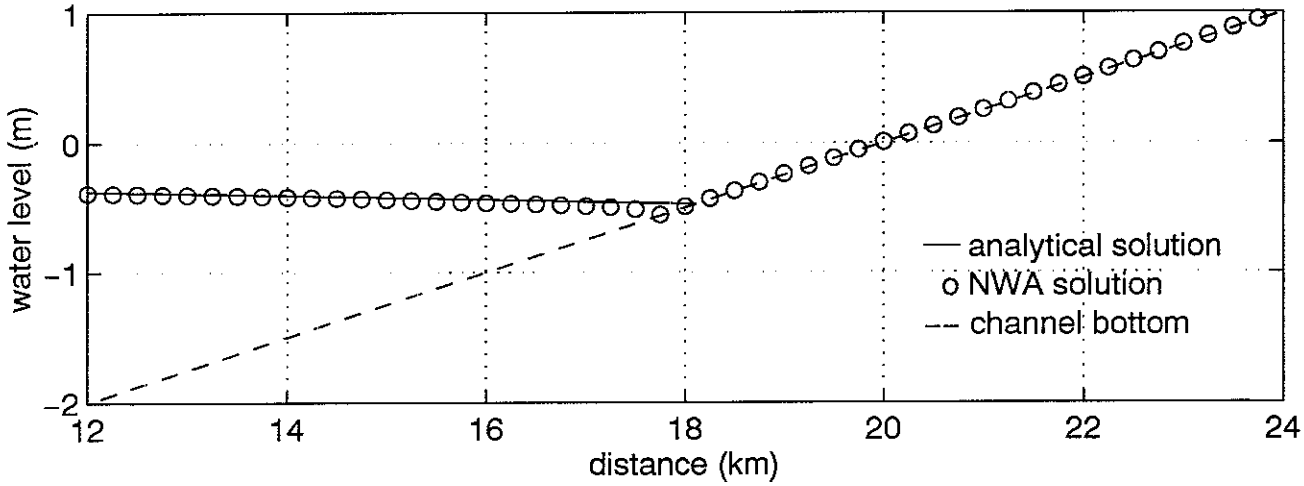

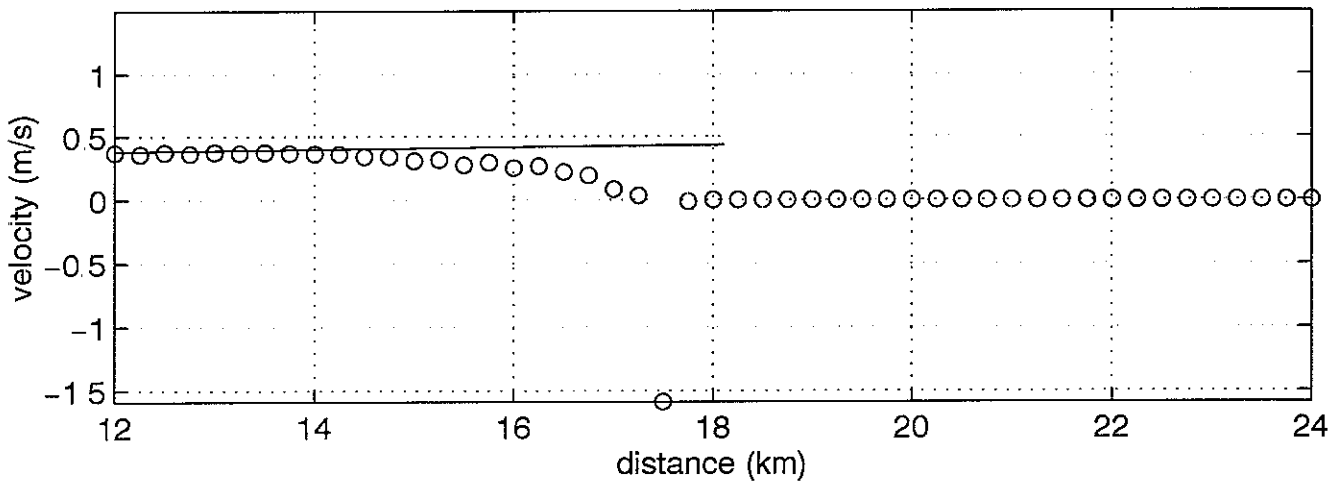

Figure 2h. Frictionless Test Case, Time = 7*T/10

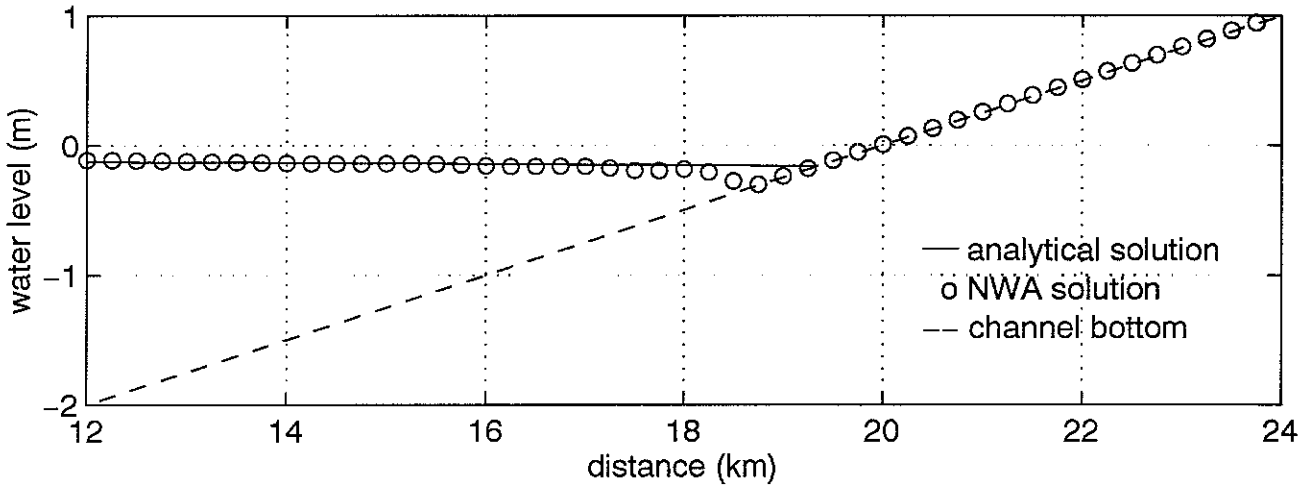

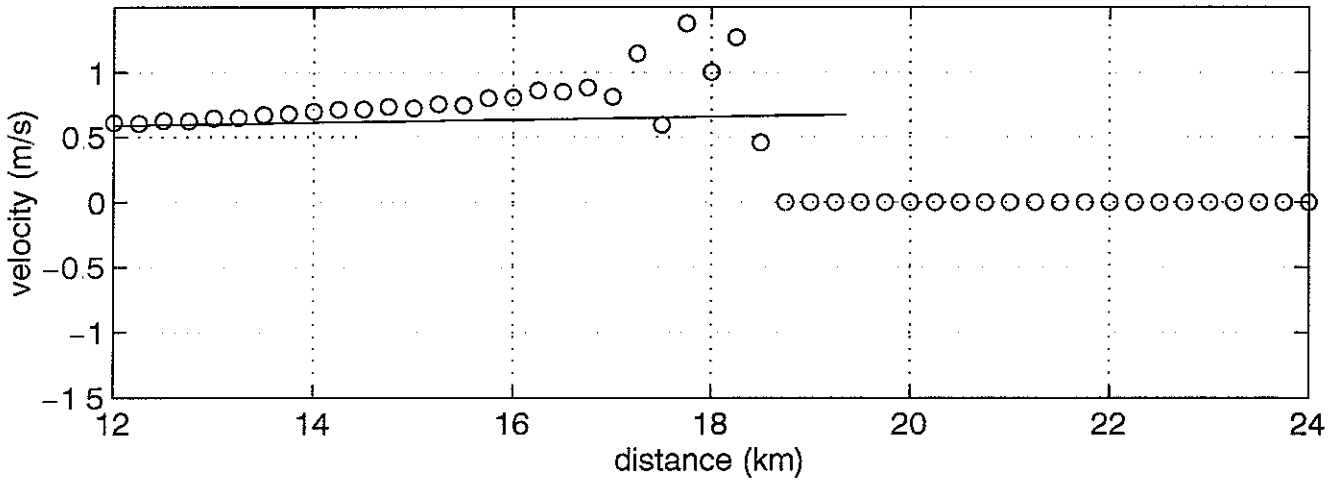

Figure 2i. Frictionless Test Case, Time = 8*T/10

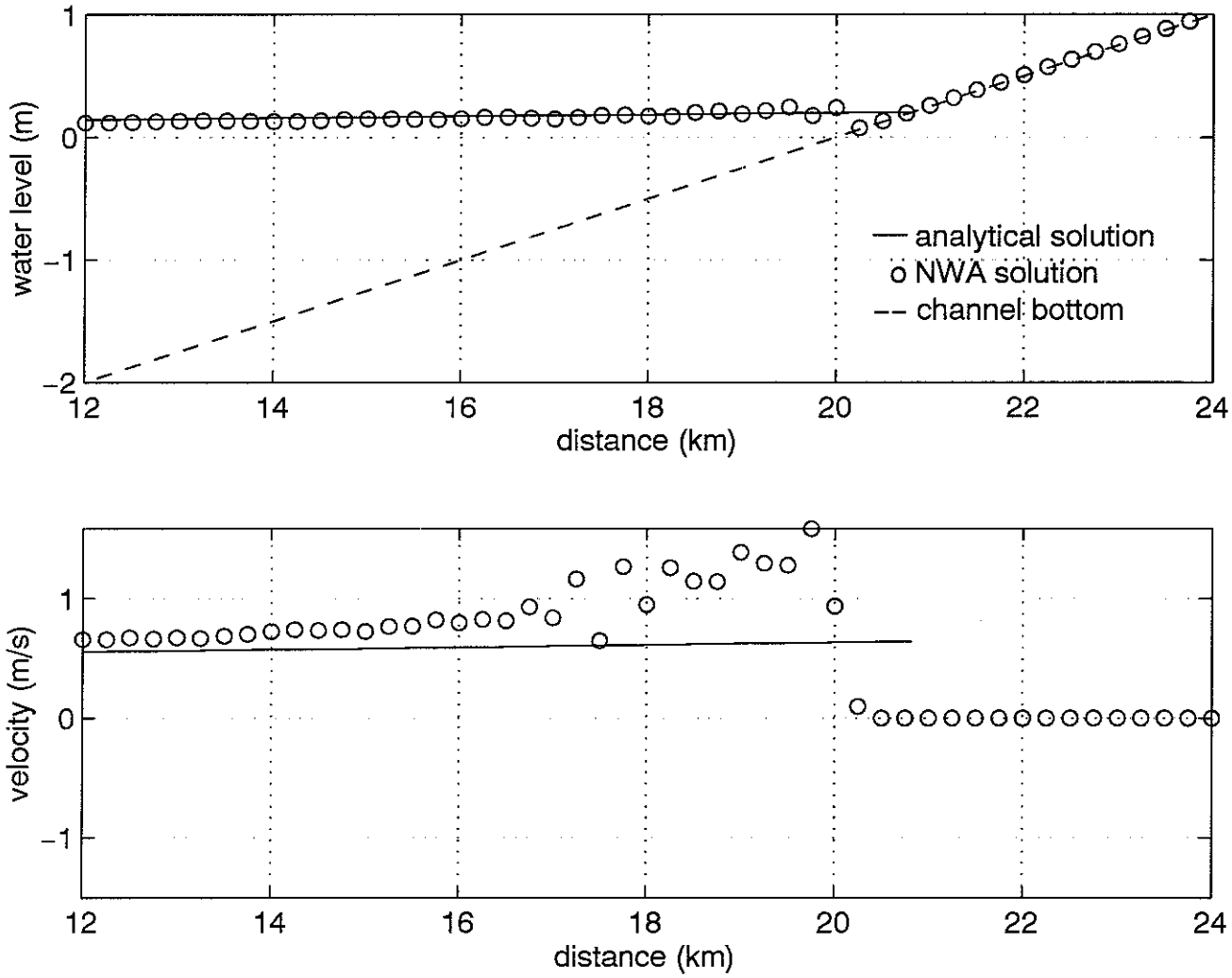

Figure 2j. Frictionless Test Case, Time = 9*T/10

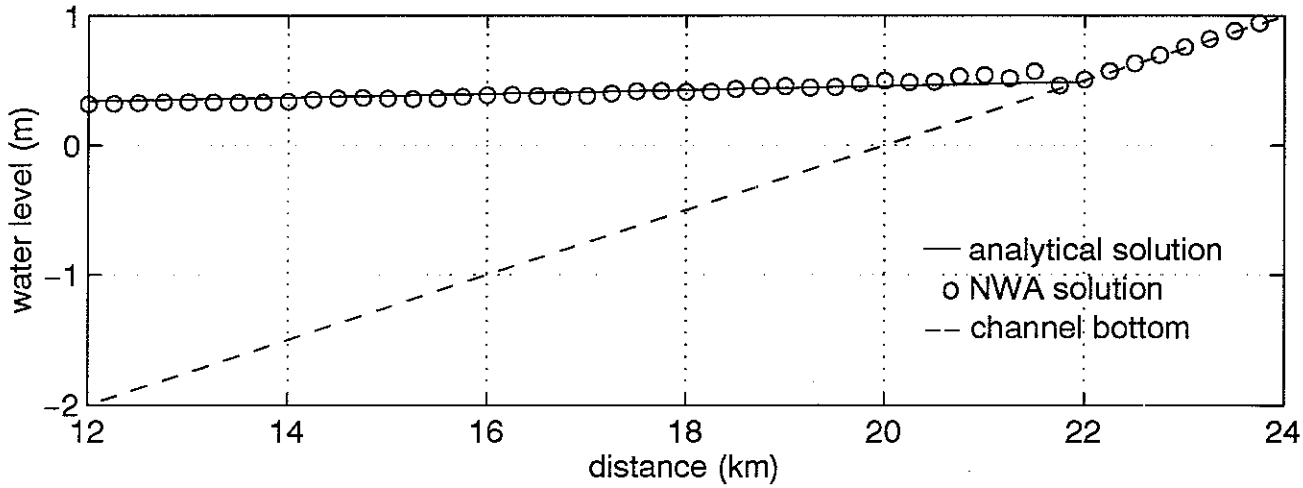

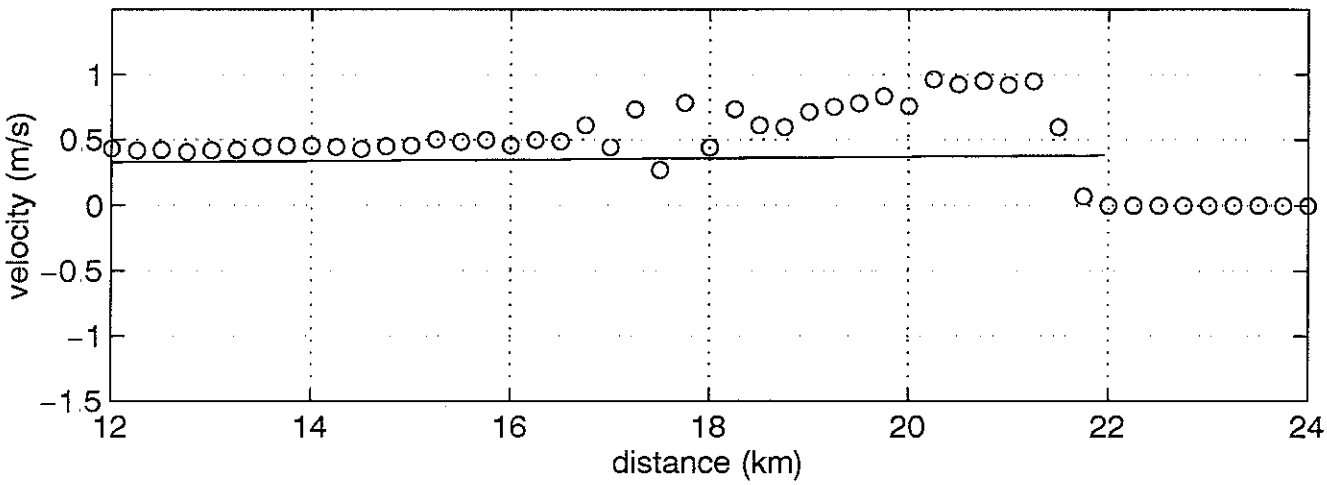

Figure 3a. Frictional Test Case #1, Time = 0*T/10

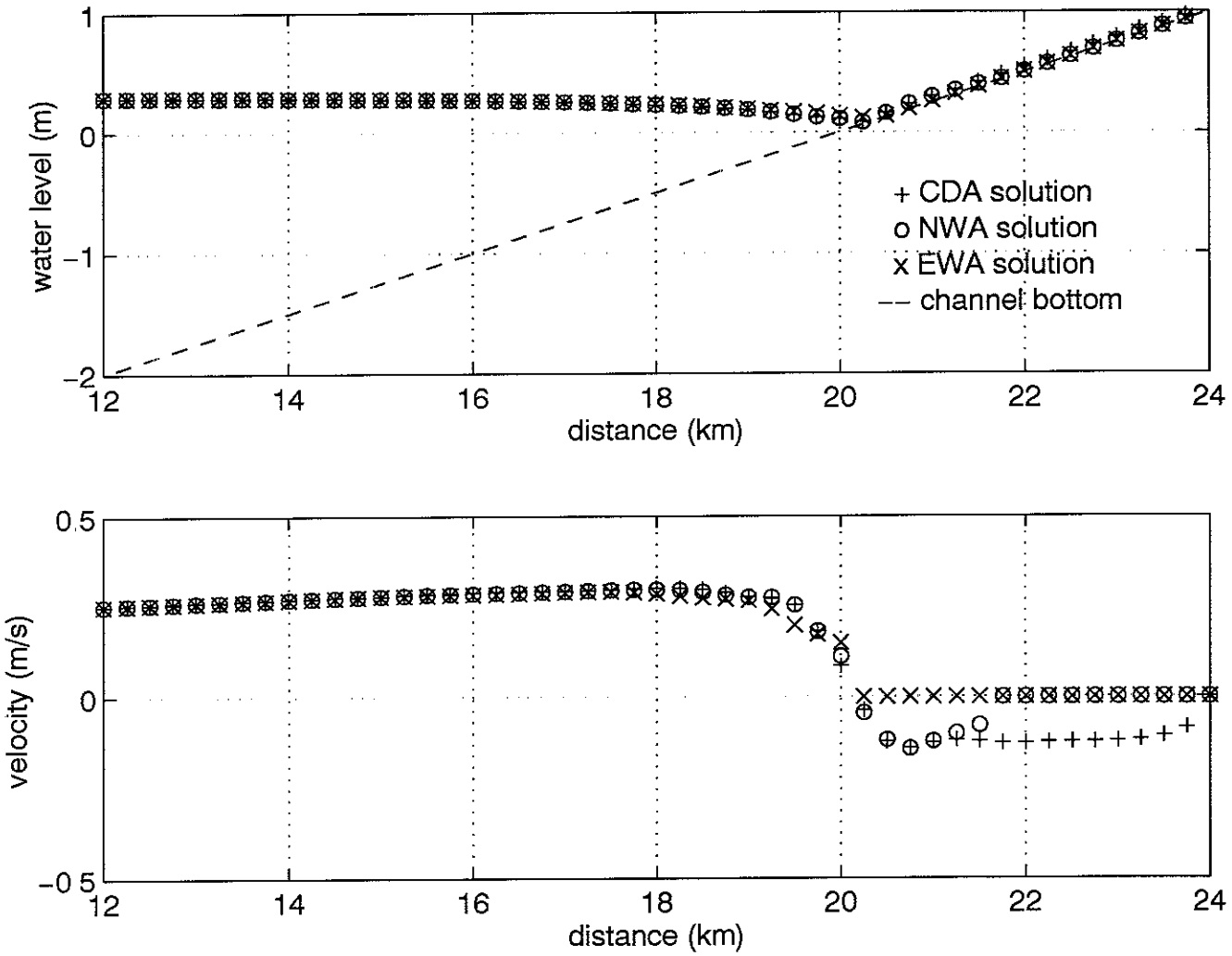

Figure 3b. Frictional Test Case #1, Time = 1*T/10

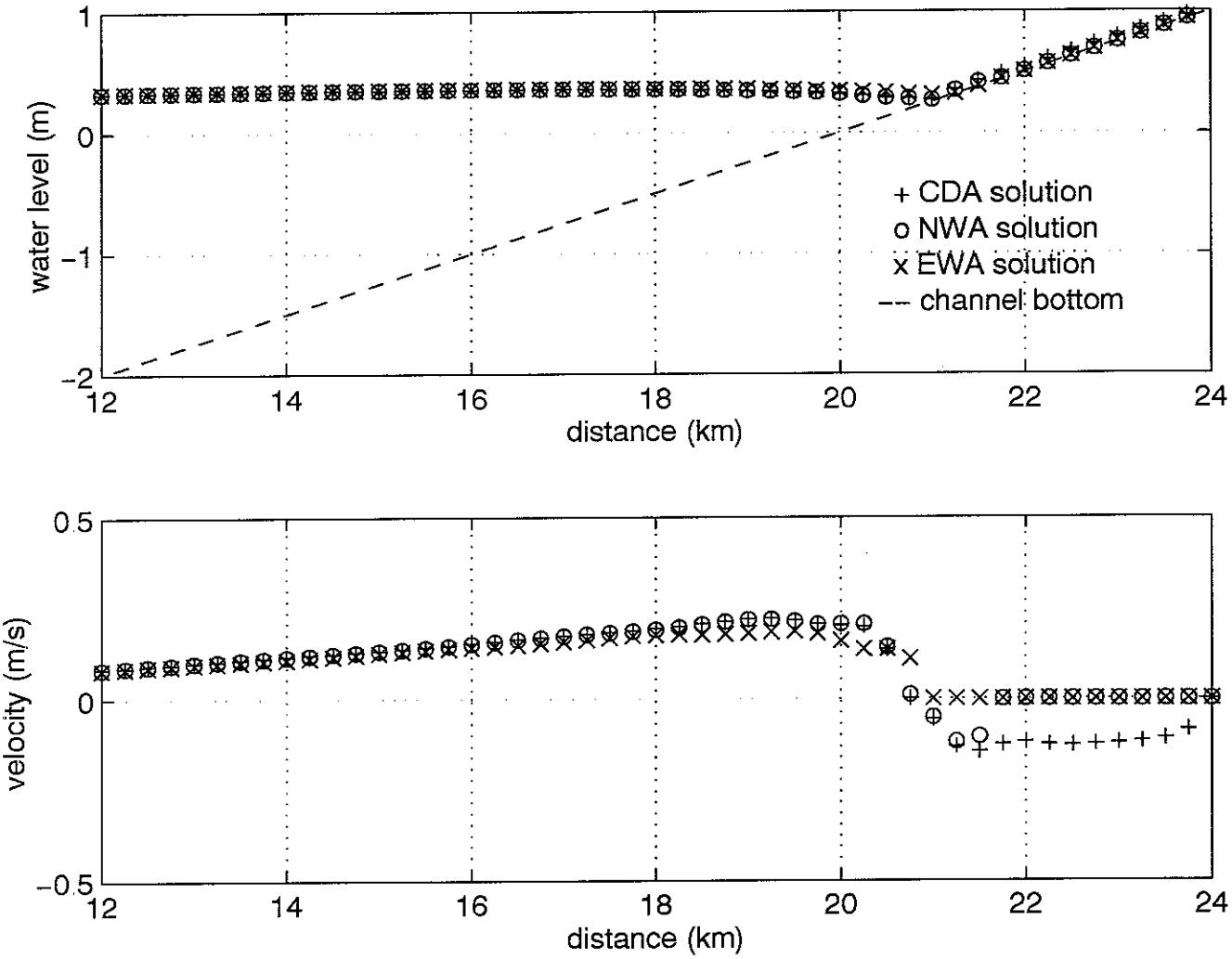

Figure 3c. Frictional Test Case #1, Time = 2*T/10

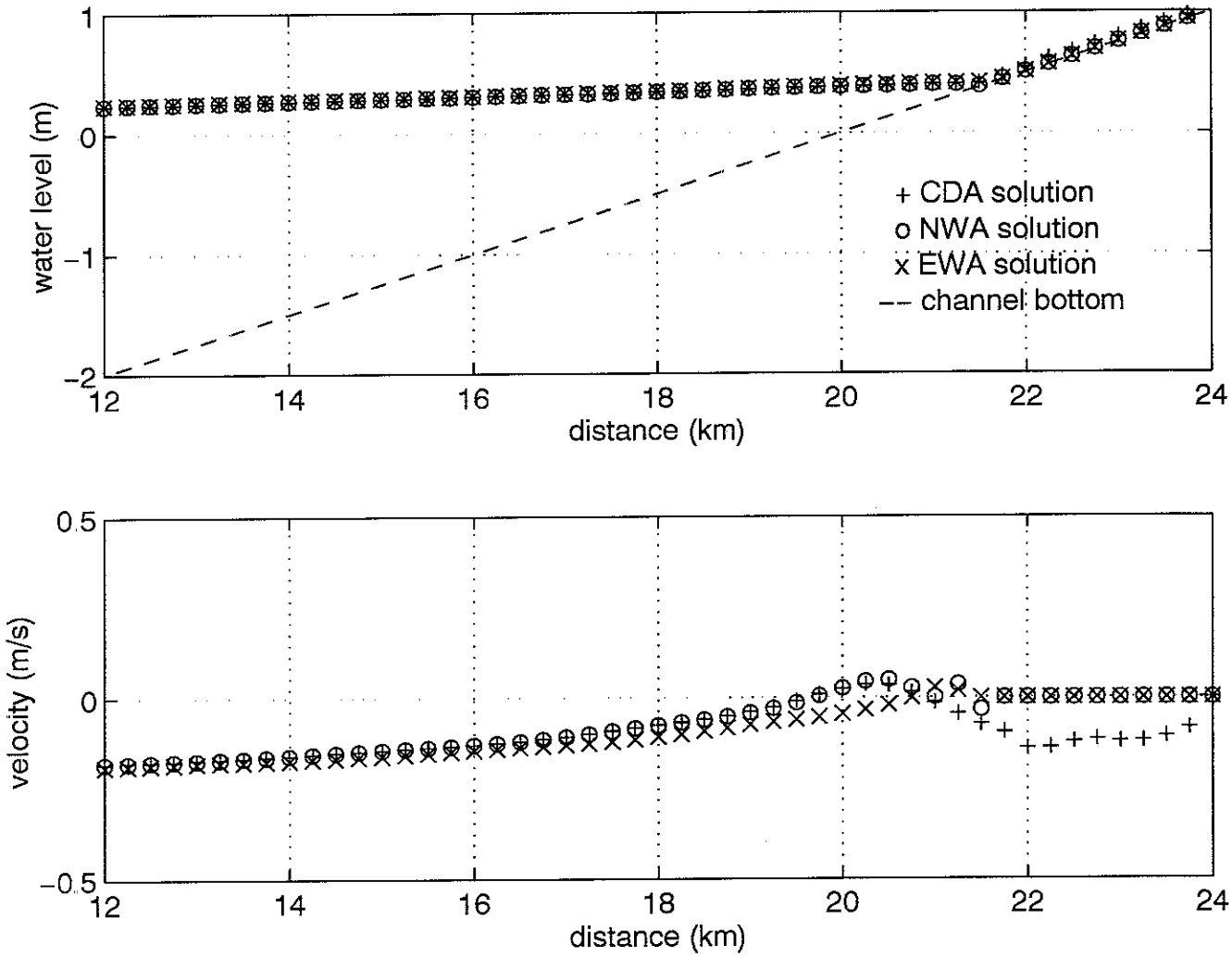

Figure 3d. Frictional Test Case #1, Time = 3*T/10

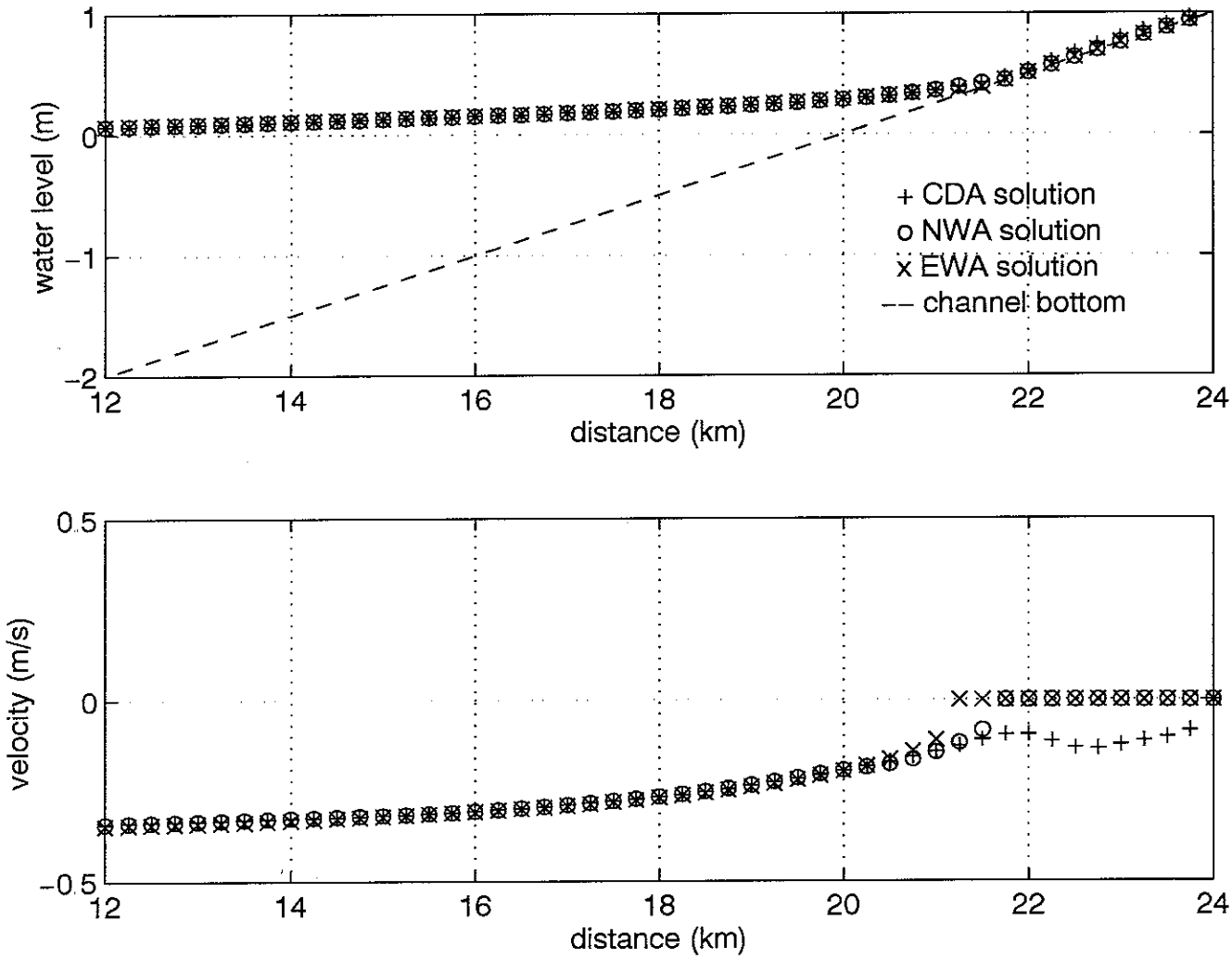

Figure 3e Frictional Test Case #1, Time = 4*T/10

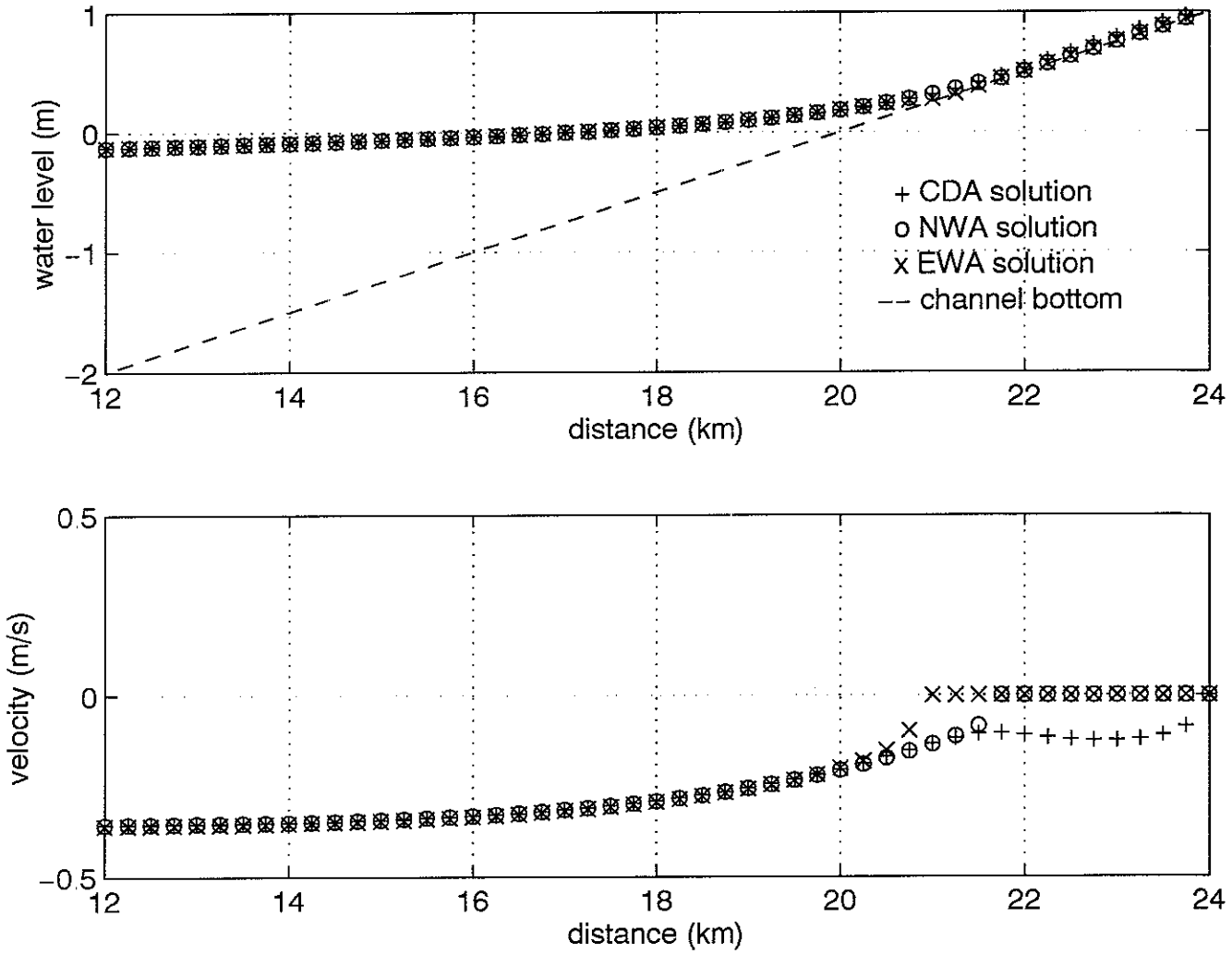

Figure 3f. Frictional Test Case #1, Time = 5*T/10

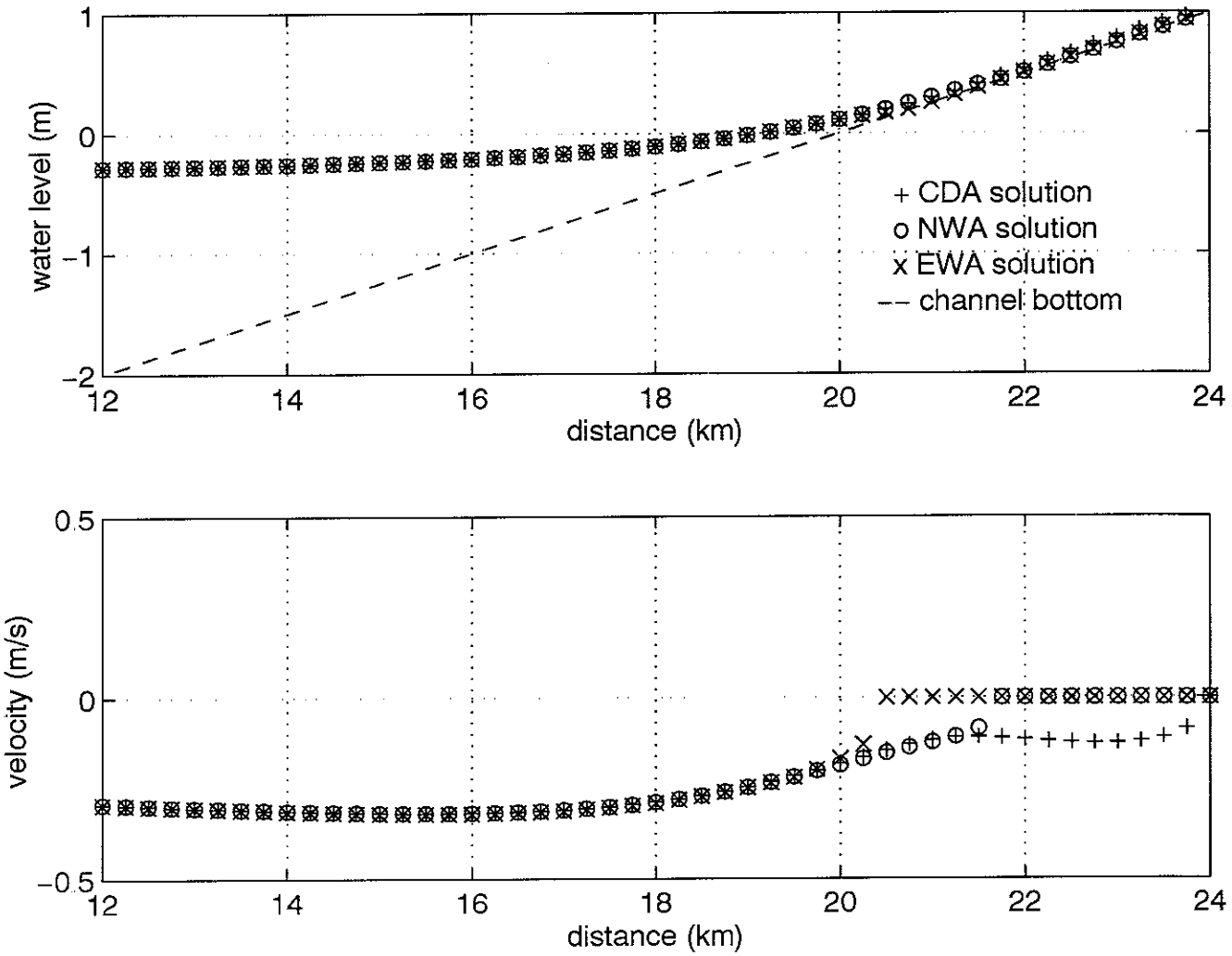

Figure 3g. Frictional Test Case #1, Time = 6*T/10

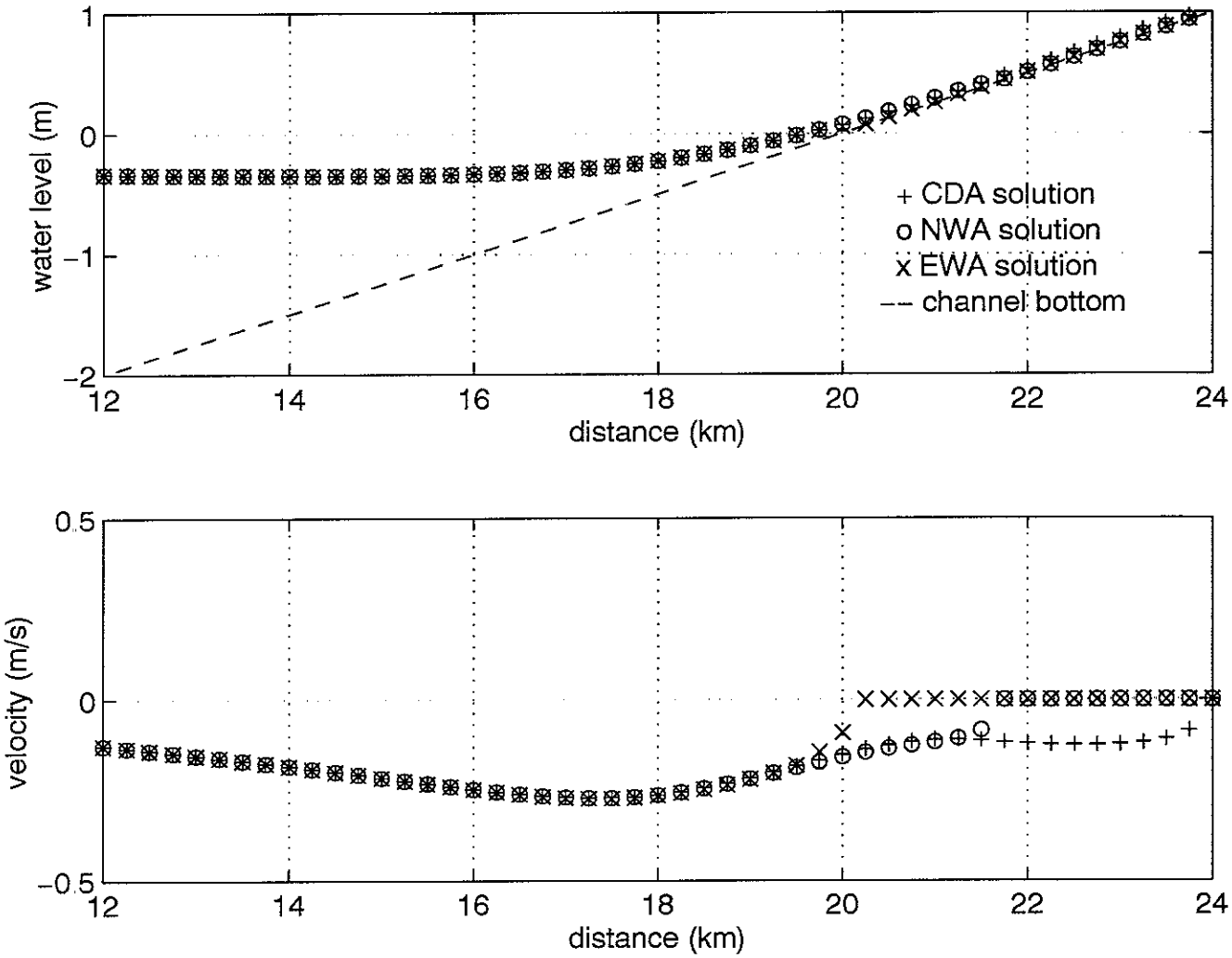

Figure 3h. Frictional Test Case #1, Time = 7*T/10

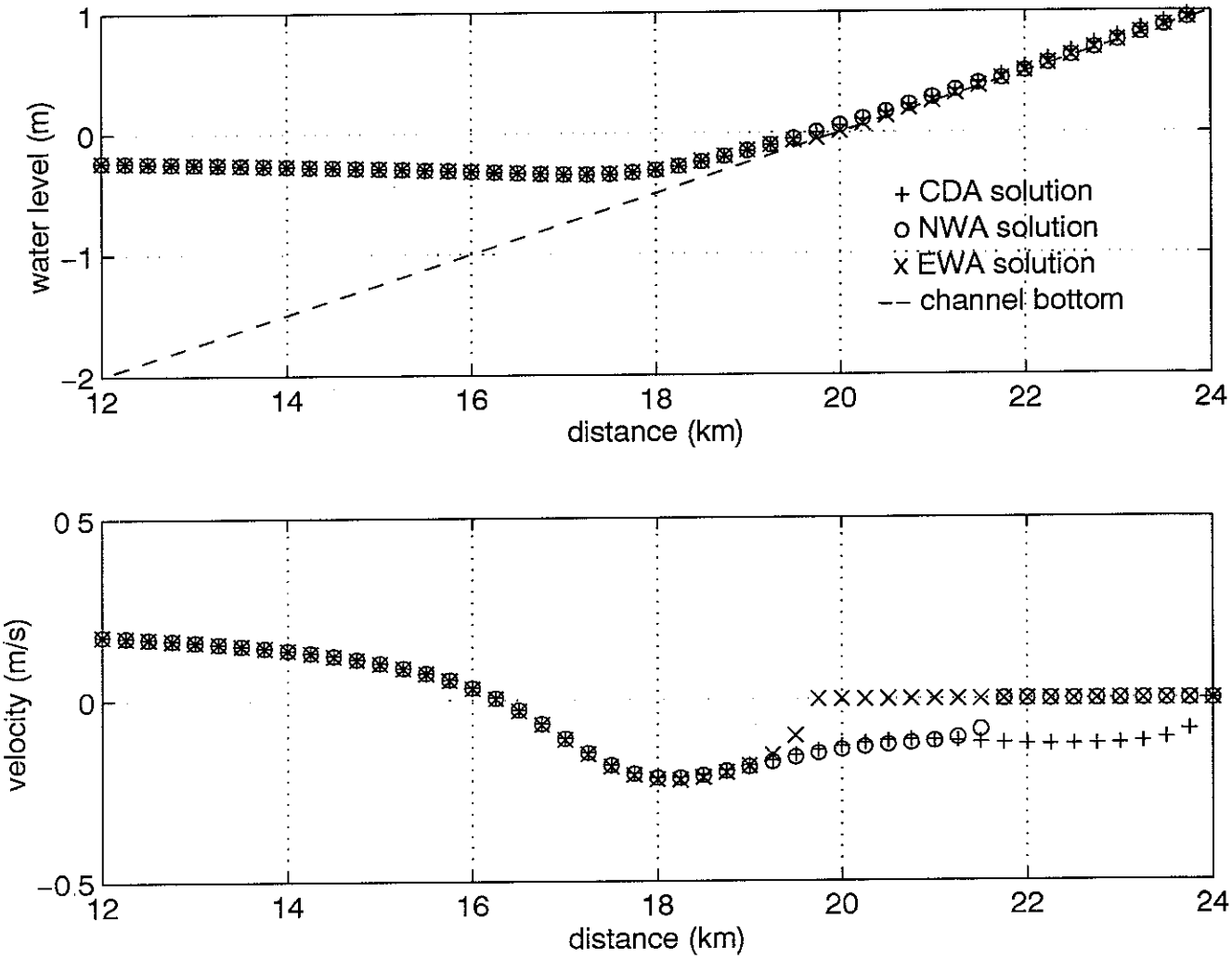

Figure 3i. Frictional Test Case #1, Time = 8*T/10

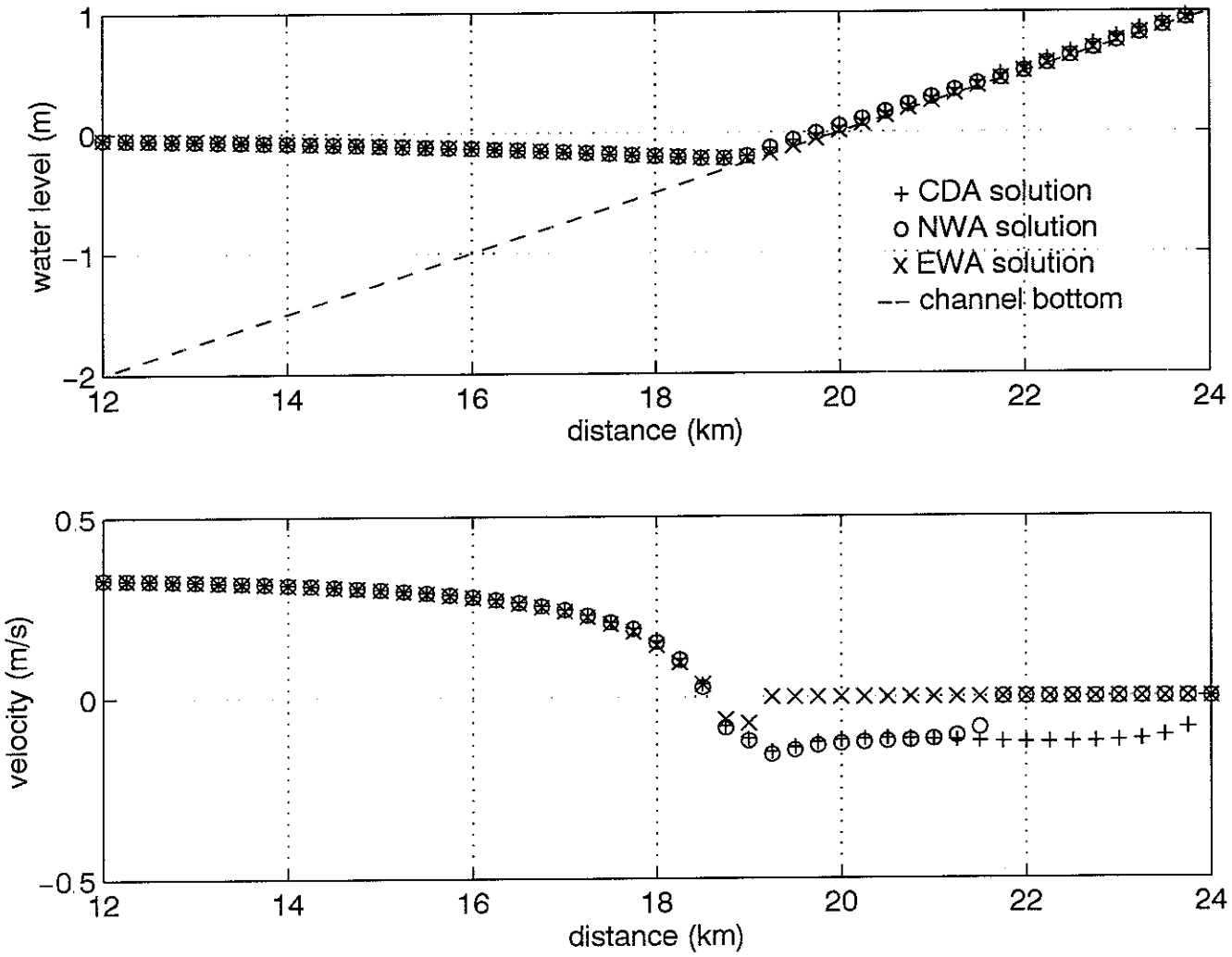

Figure 3j. Frictional Test Case #1, Time = 9*T/10

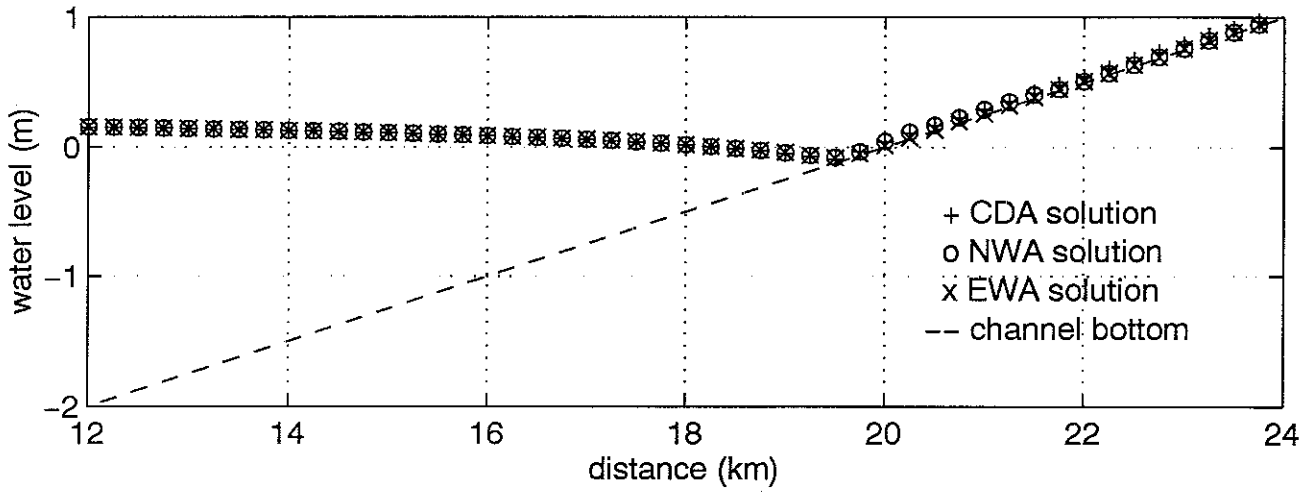

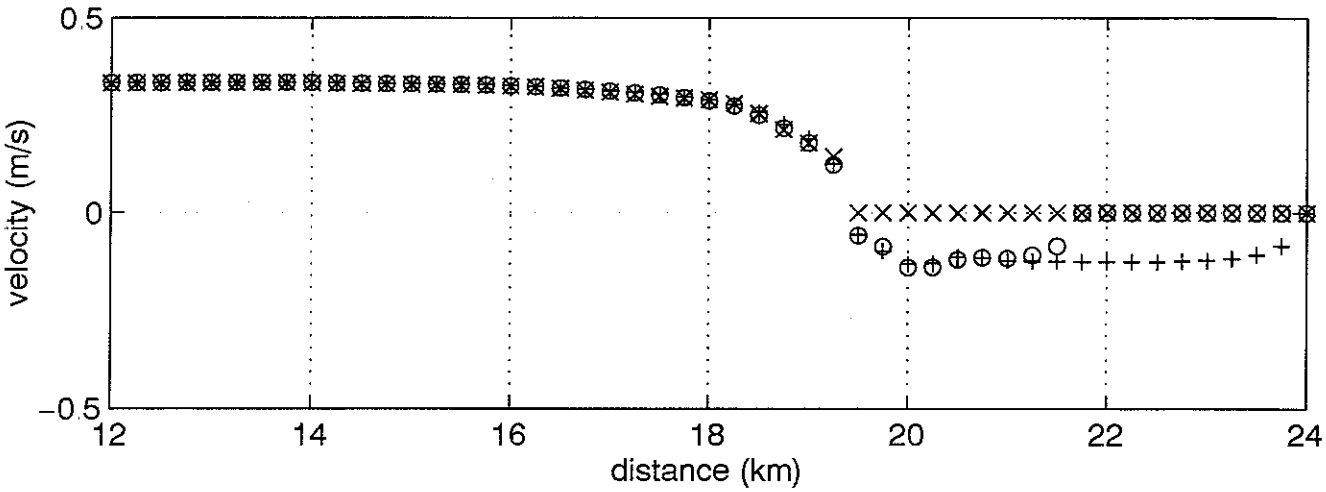

Figure 4a. Frictional Test Case #2, Time = 0*T/10

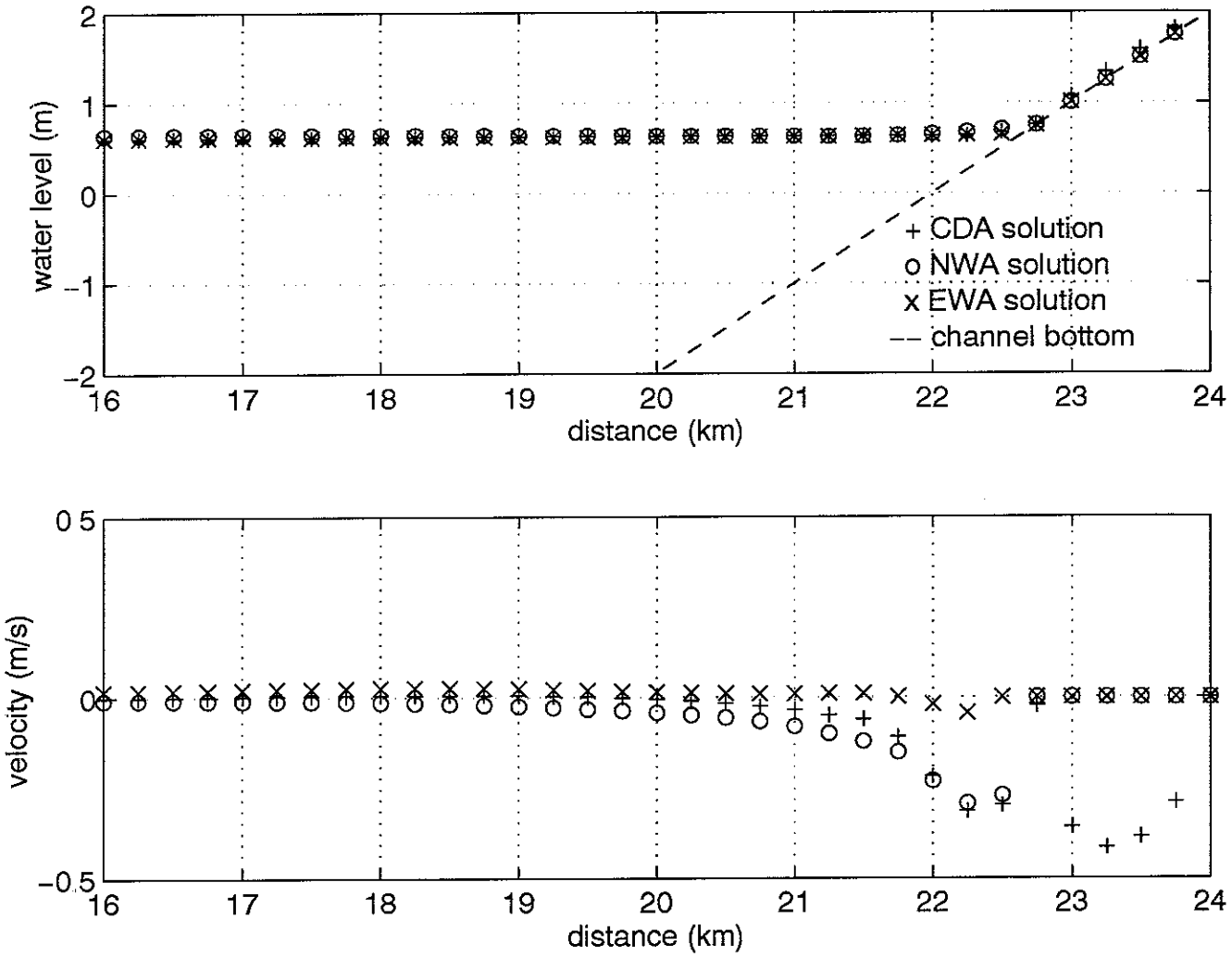

Figure 4b. Frictional Test Case #2, Time = 1*T/10

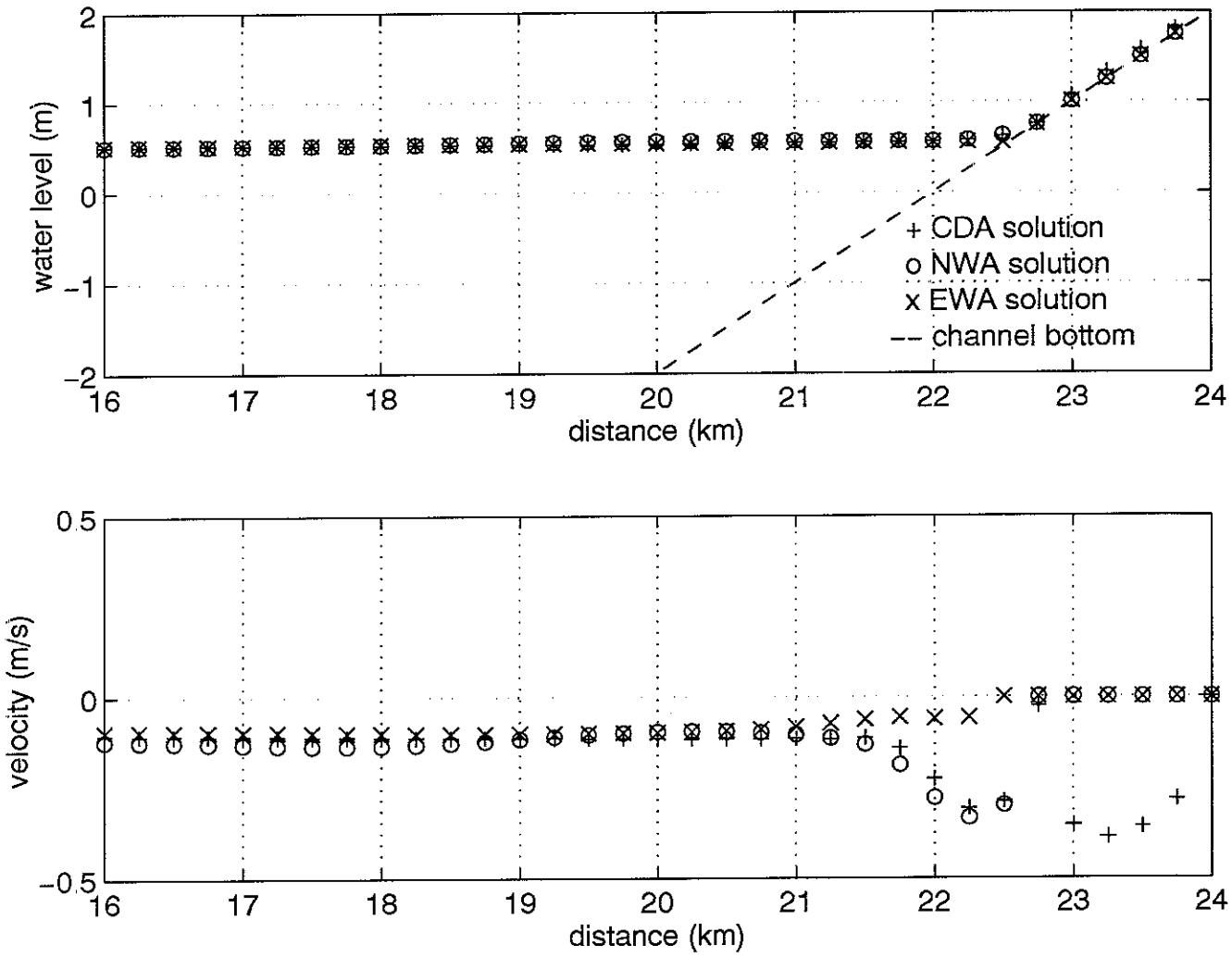

Figure 4c. Frictional Test Case #2, Time = 2*T/10

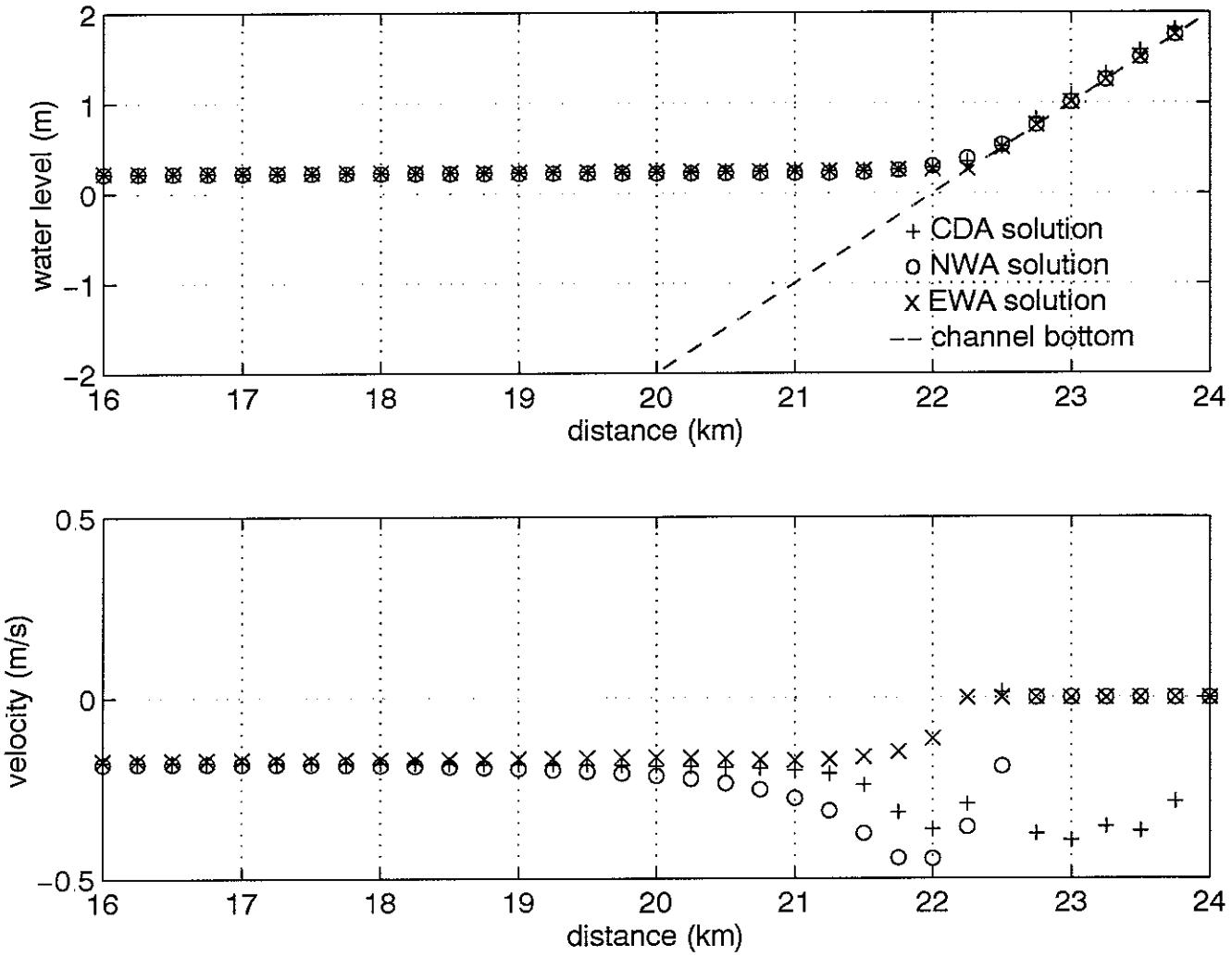

Figure 4d. Frictional Test Case #2, Time = 3*T/10

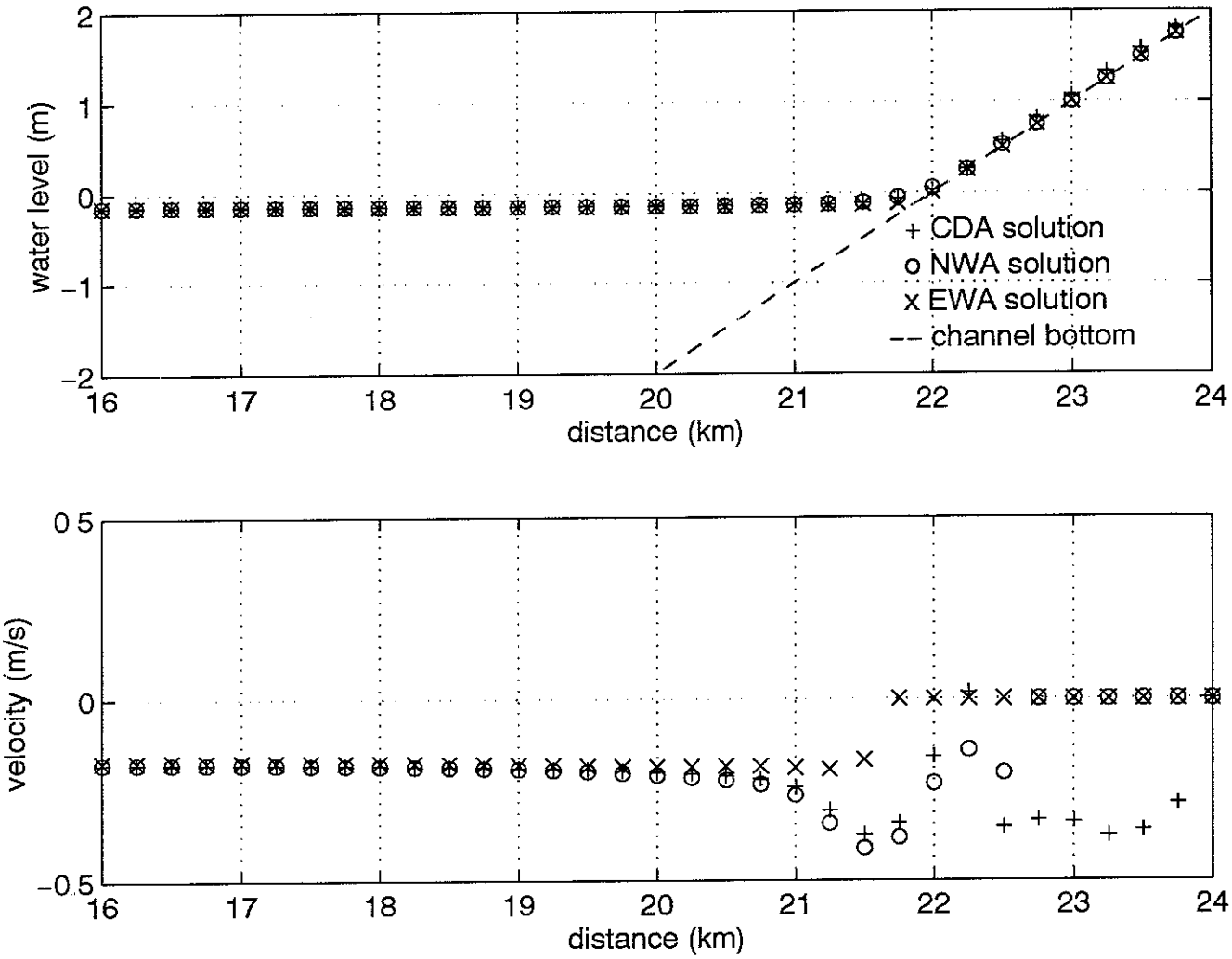

Figure 4e. Frictional Test Case #2, Time = 4*T/10

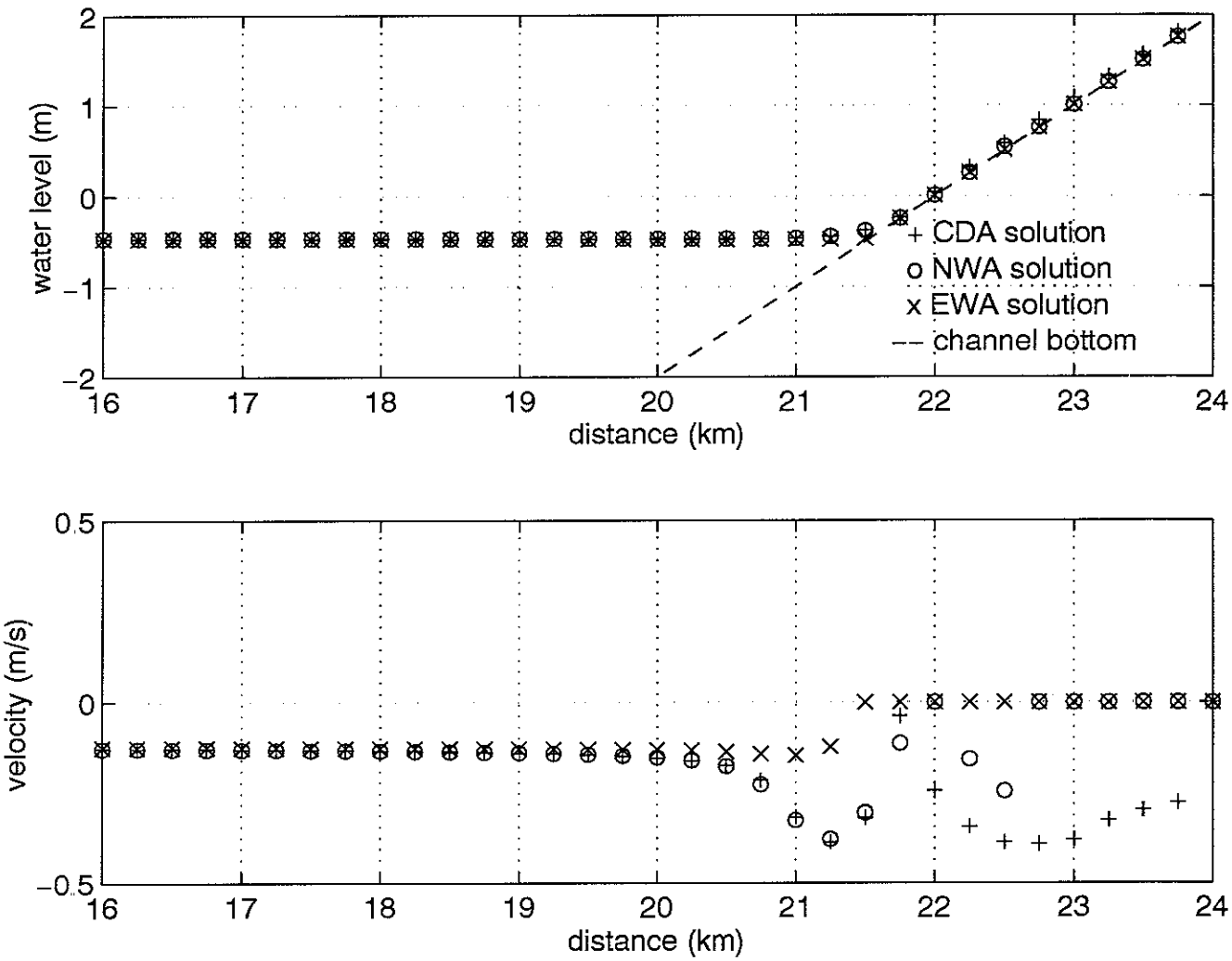

Figure 4f Frictional Test Case #2, Time = 5*T/10

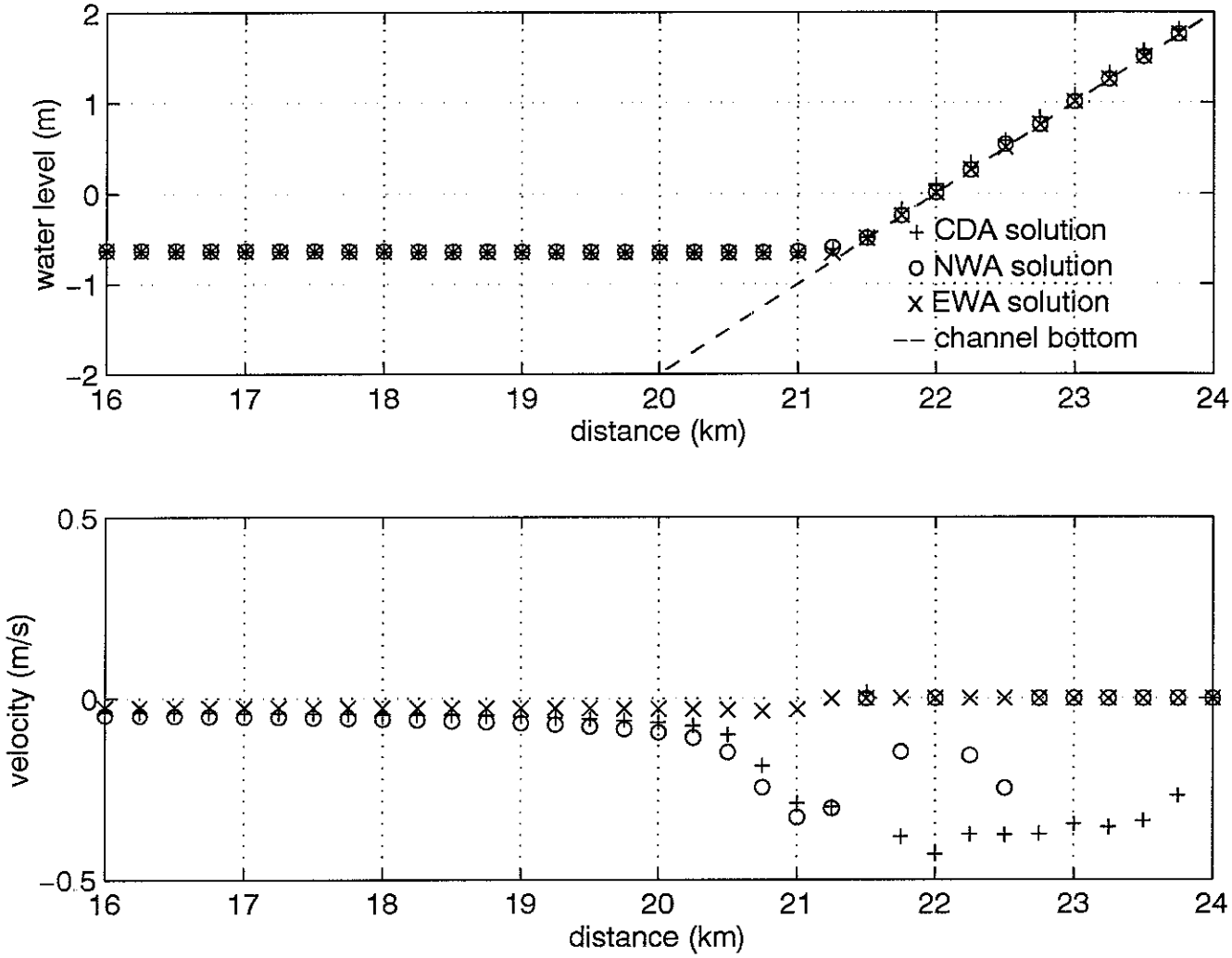

Figure 4g. Frictional Test Case #2, Time = 6*T/10

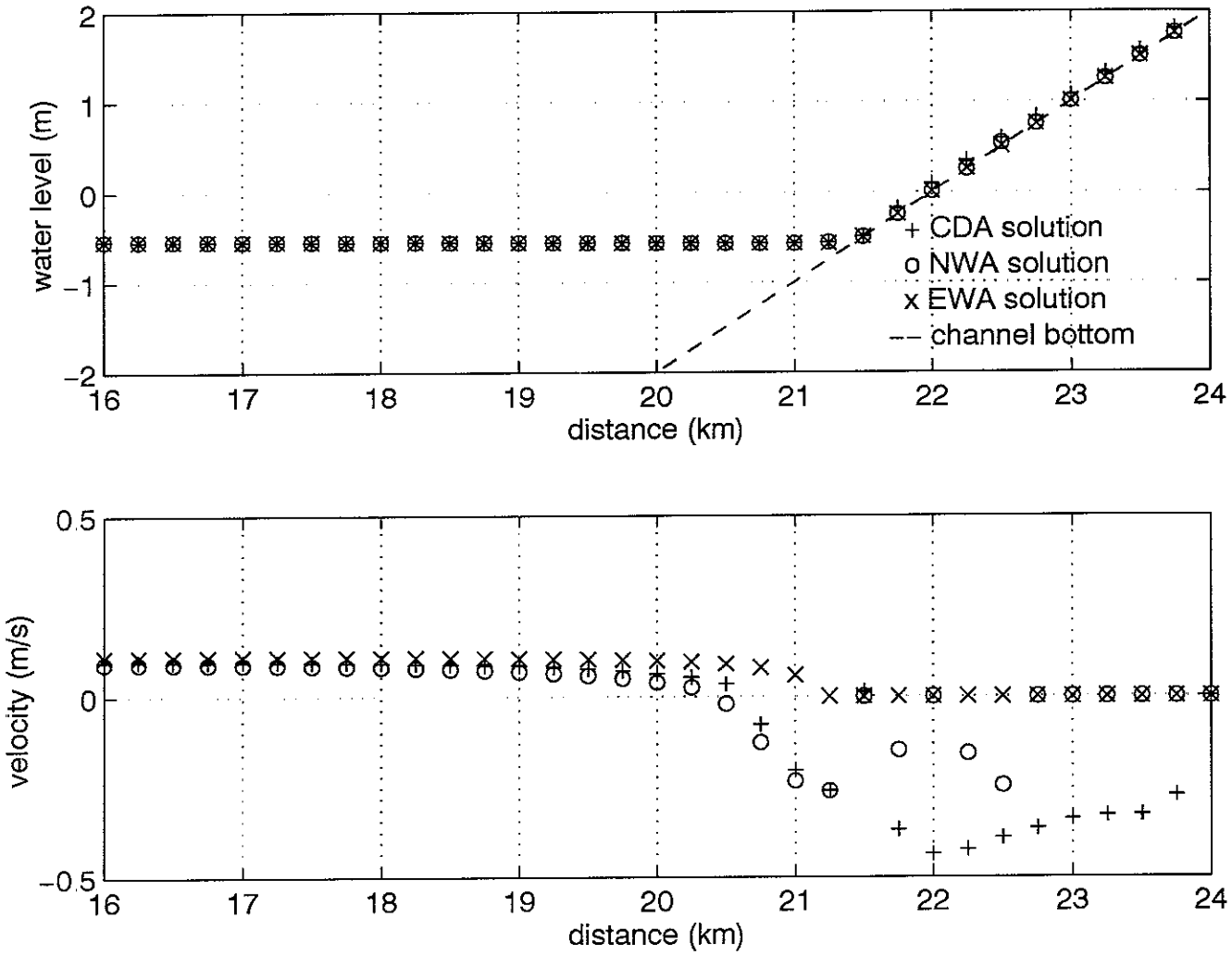

Figure 4h. Frictional Test Case #2, Time = 7*T/10

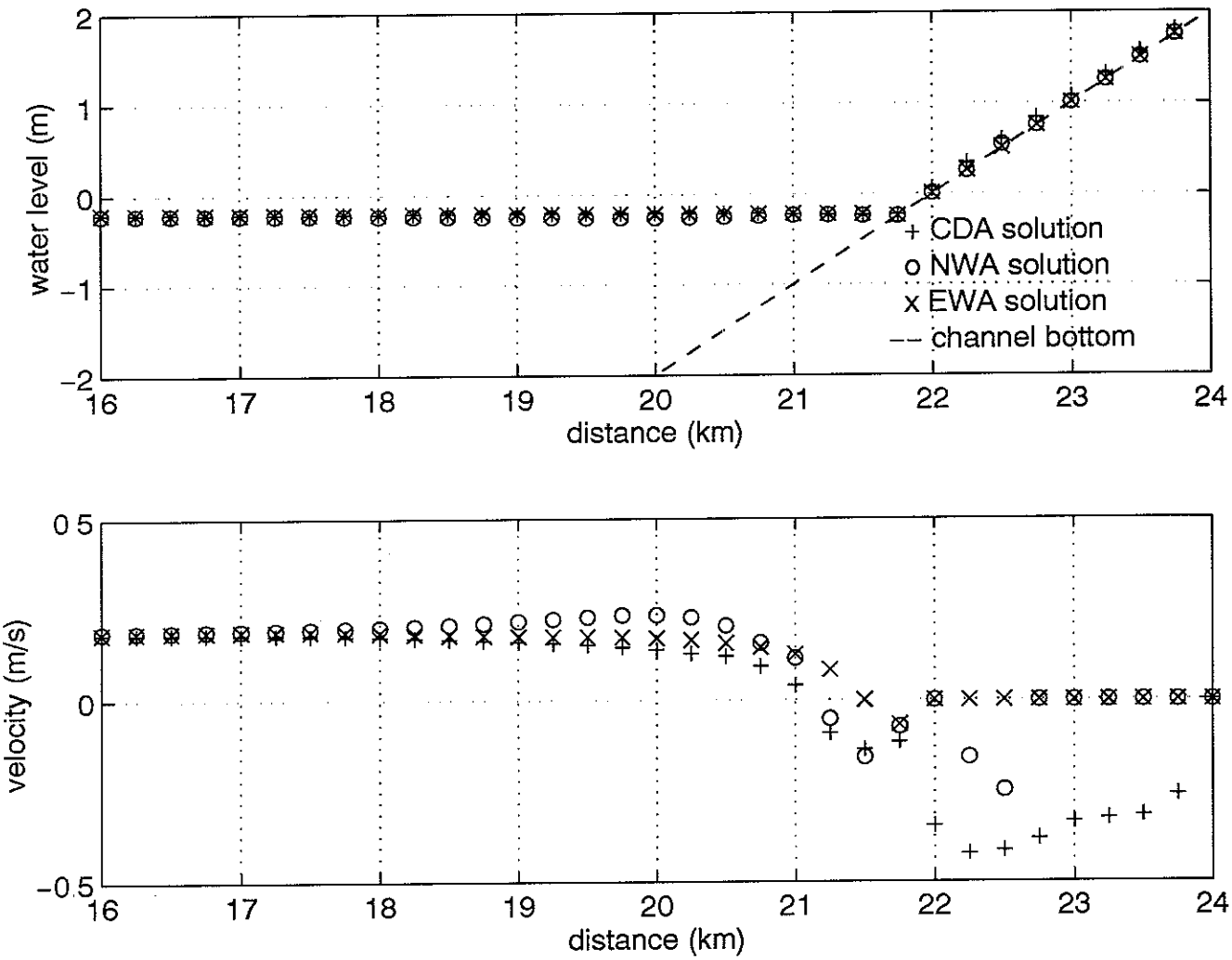

Figure 4i. Frictional Test Case #2, Time = 8*T/10

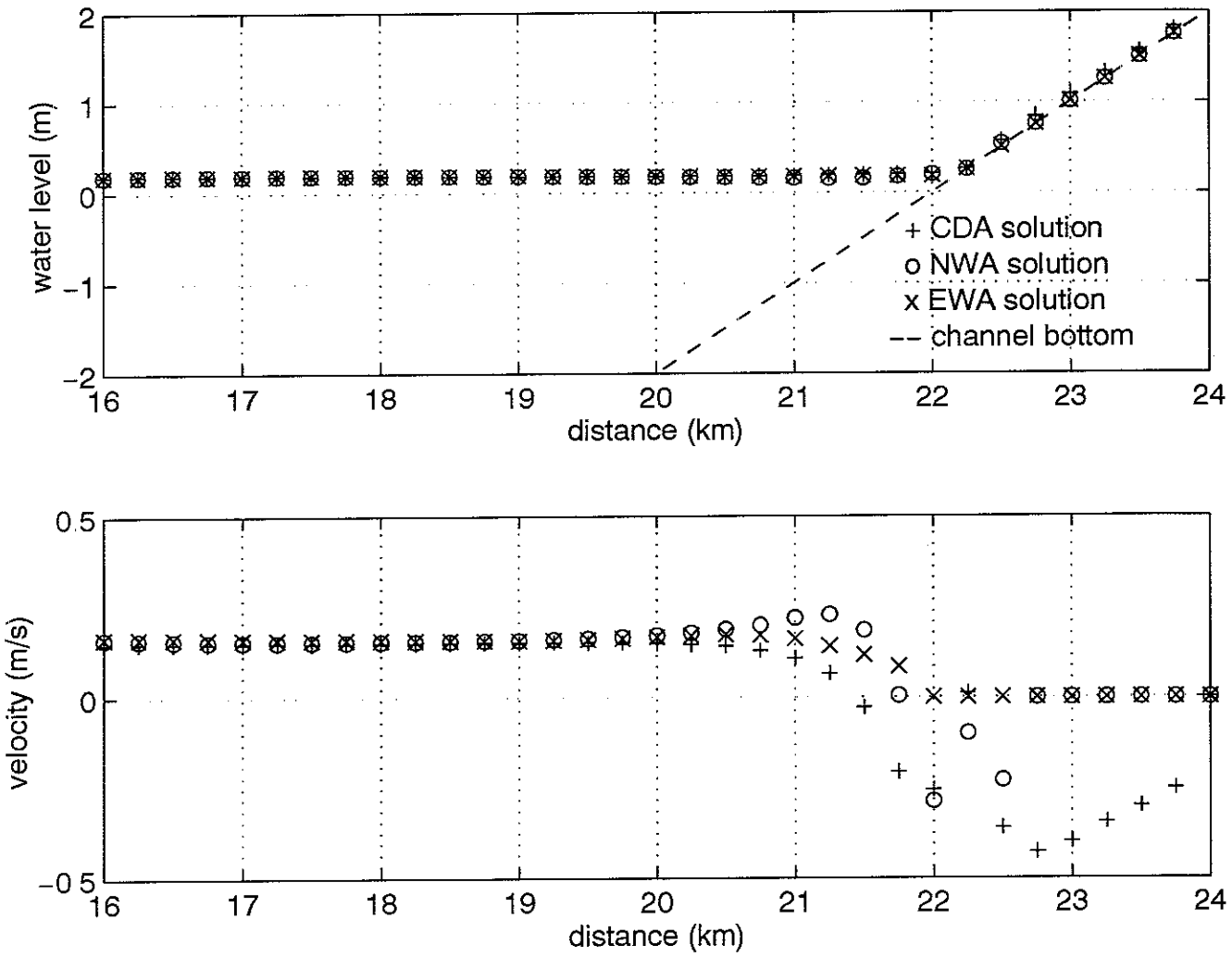

Figure 4j. Frictional Test Case #2, Time = 9*T/10

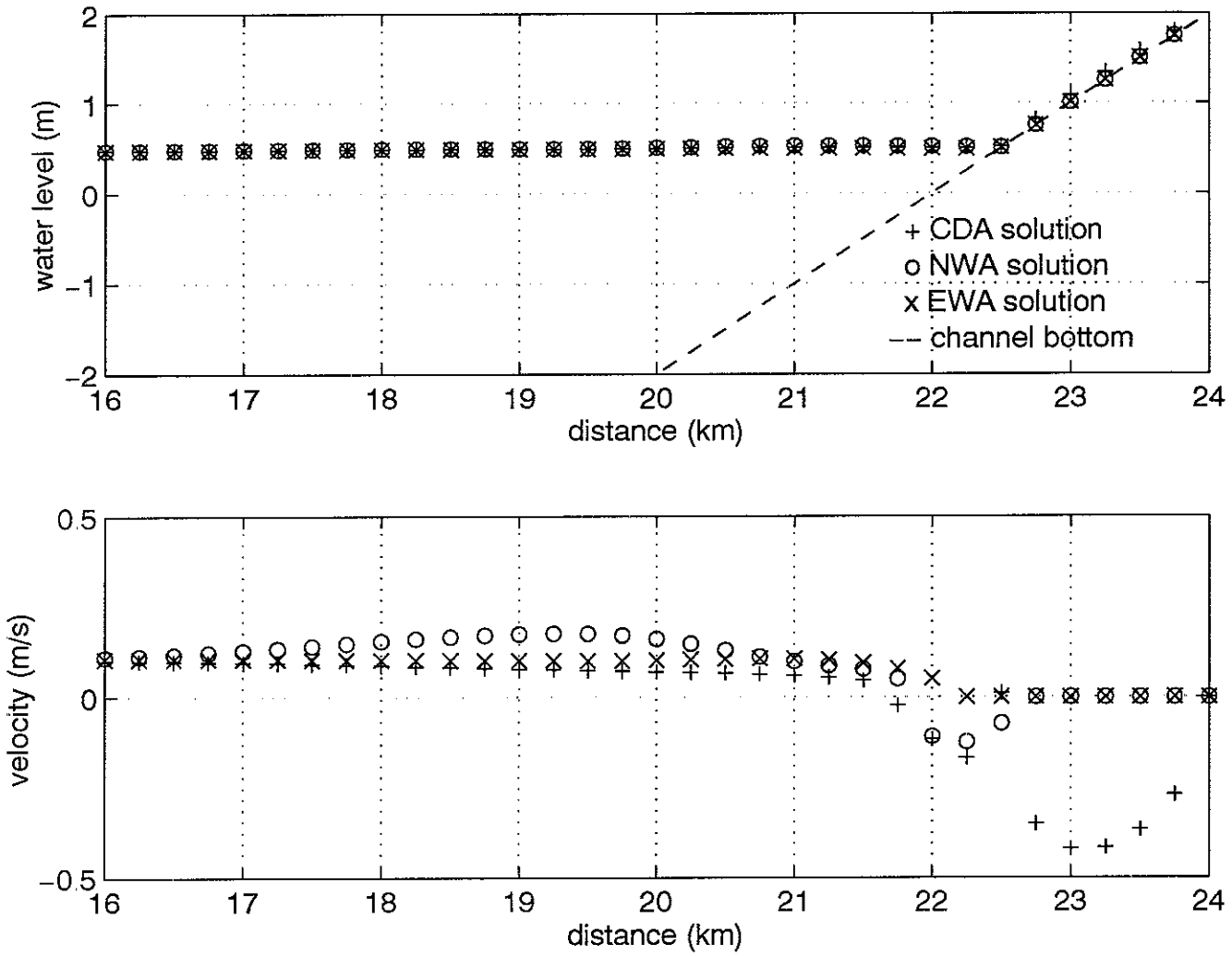

Figure 5a. Berm Test Case, Time = 0*T/10

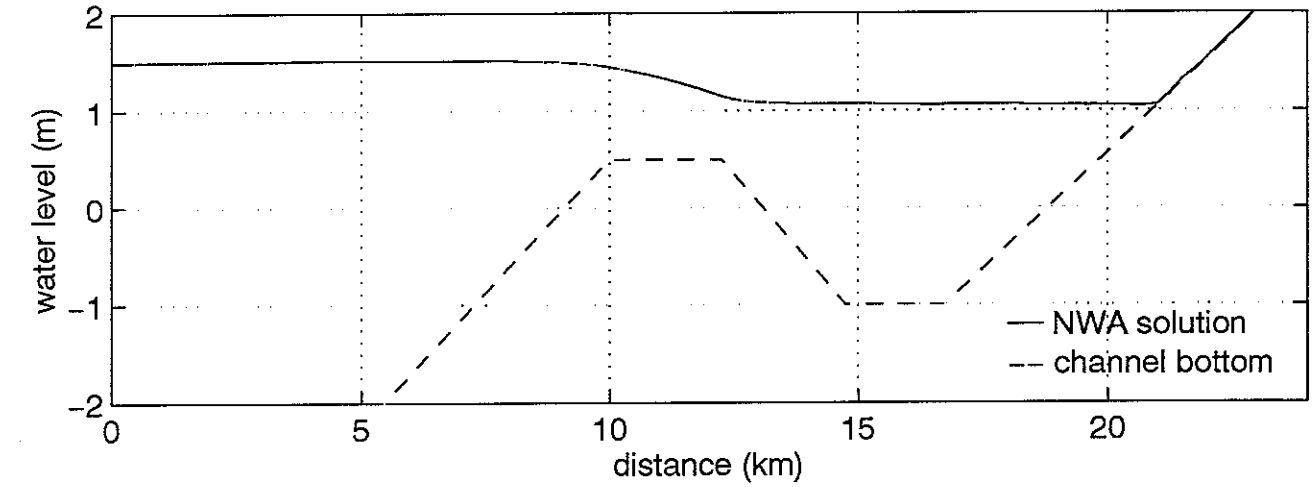

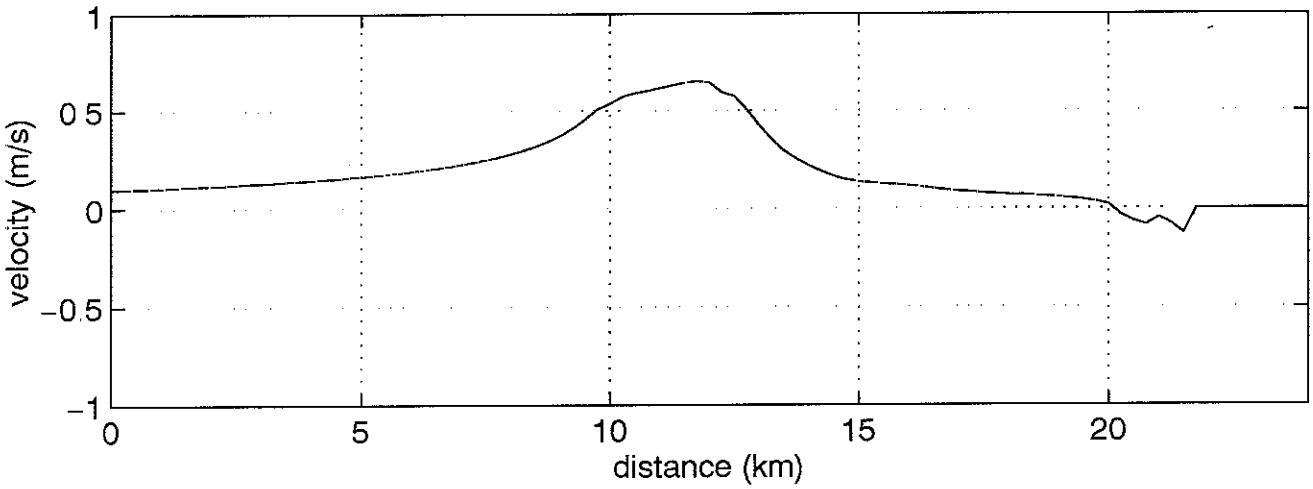

Figure 5b. Berm Test Case, Time = 1*T/10

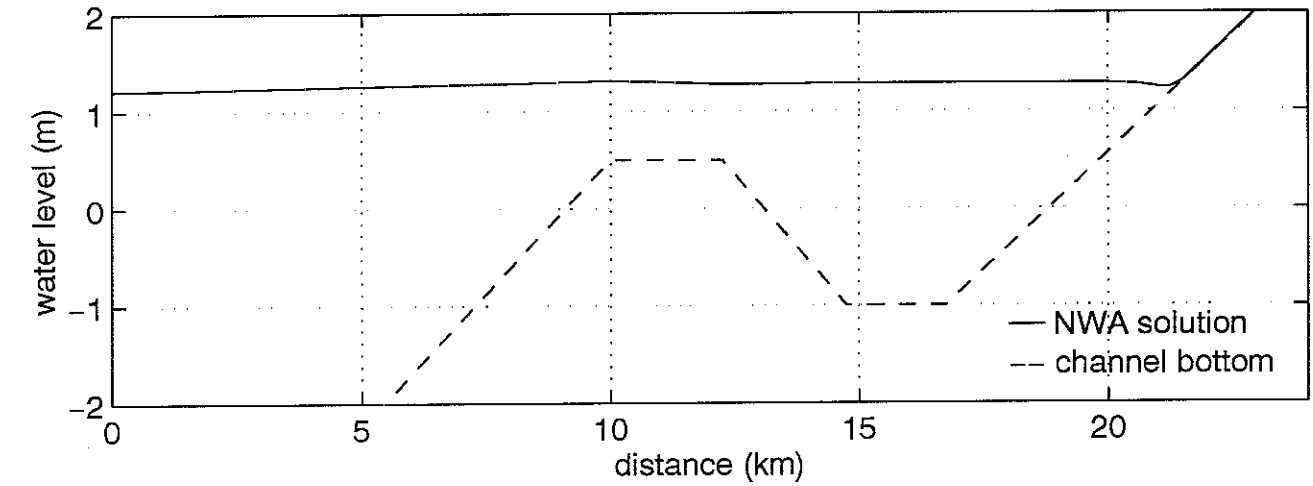

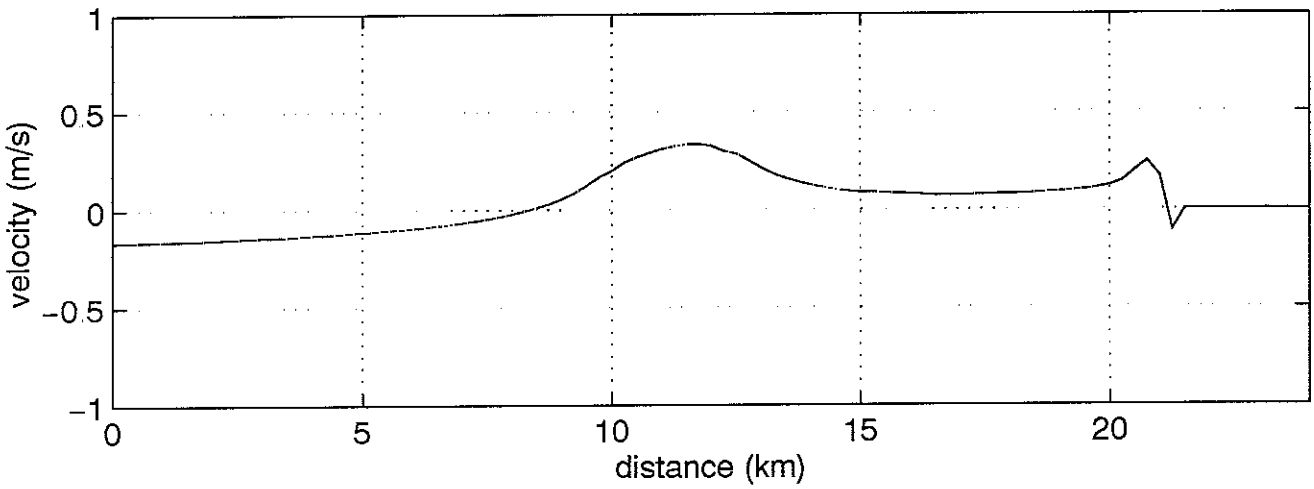

Figure 5c. Berm Test Case, Time = 2*T/10

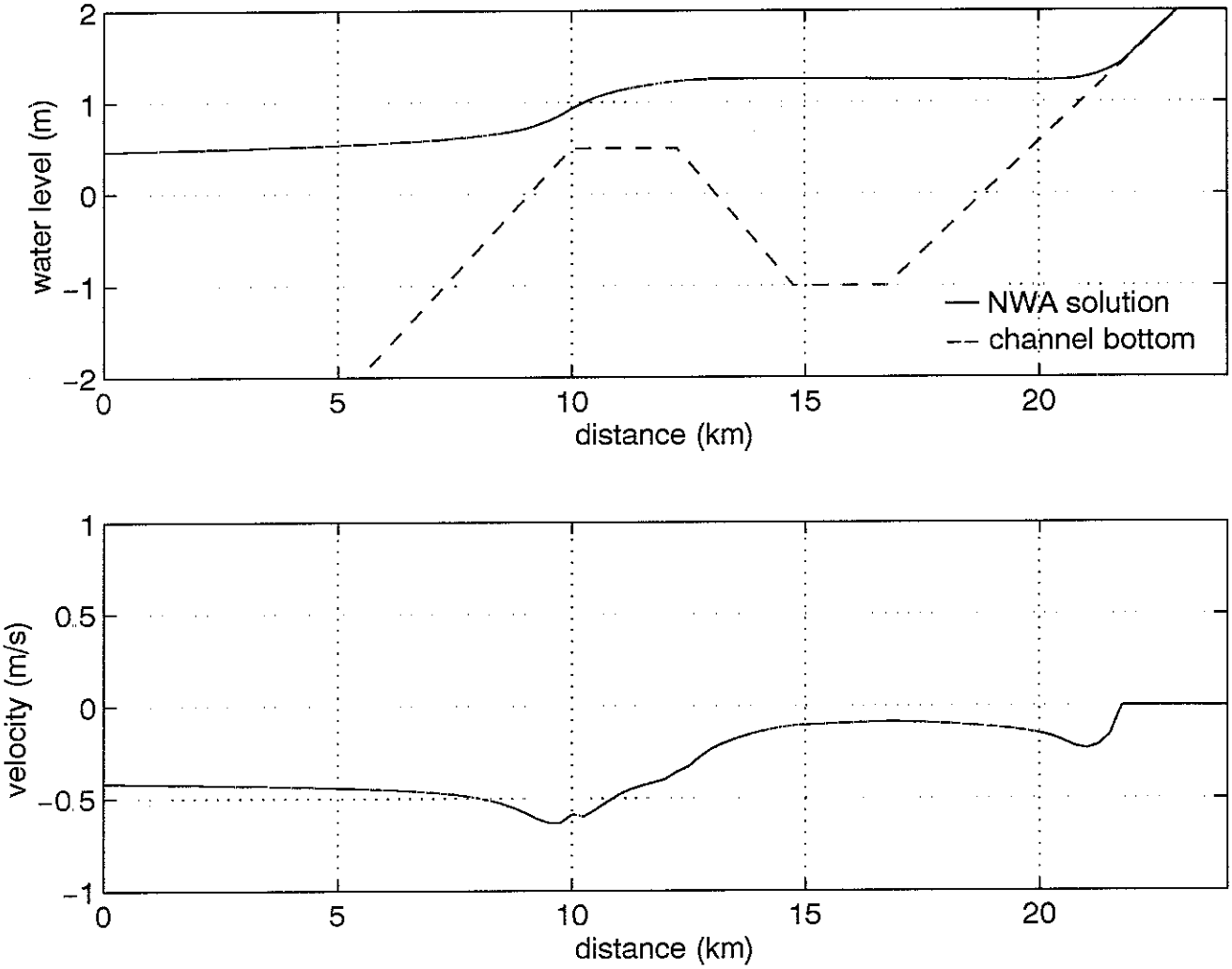

Figure 5d. Berm Test Case, Time = 3*T/10

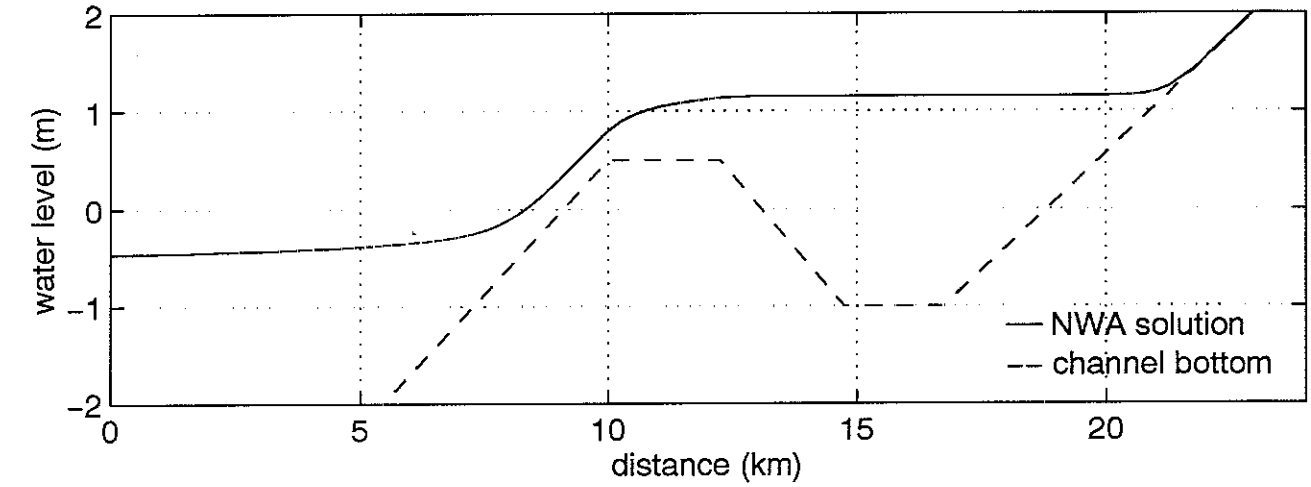

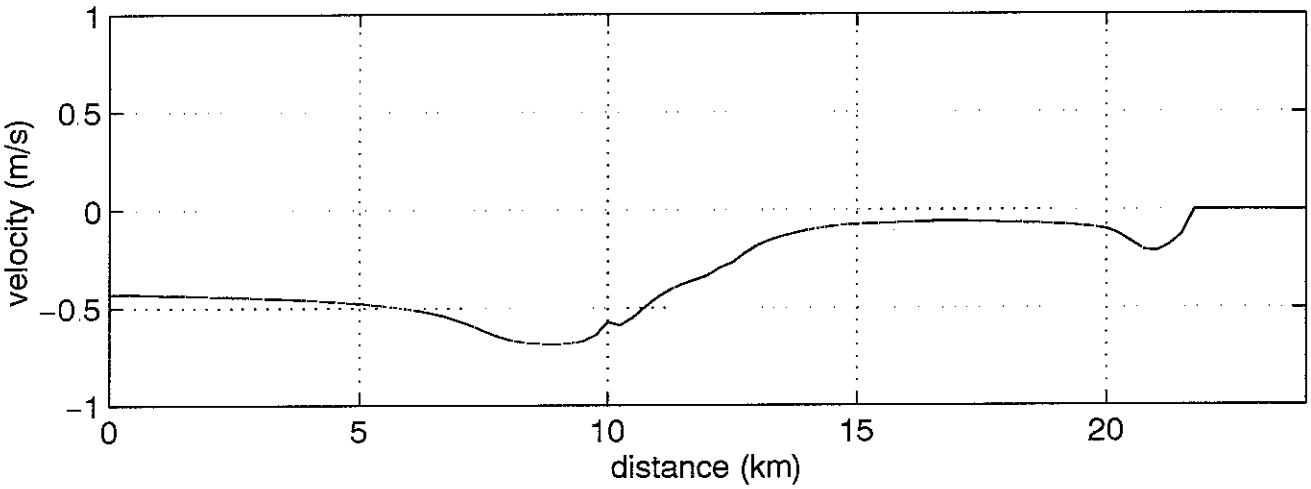

Figure 5e Berm Test Case, Time = 4*T/10

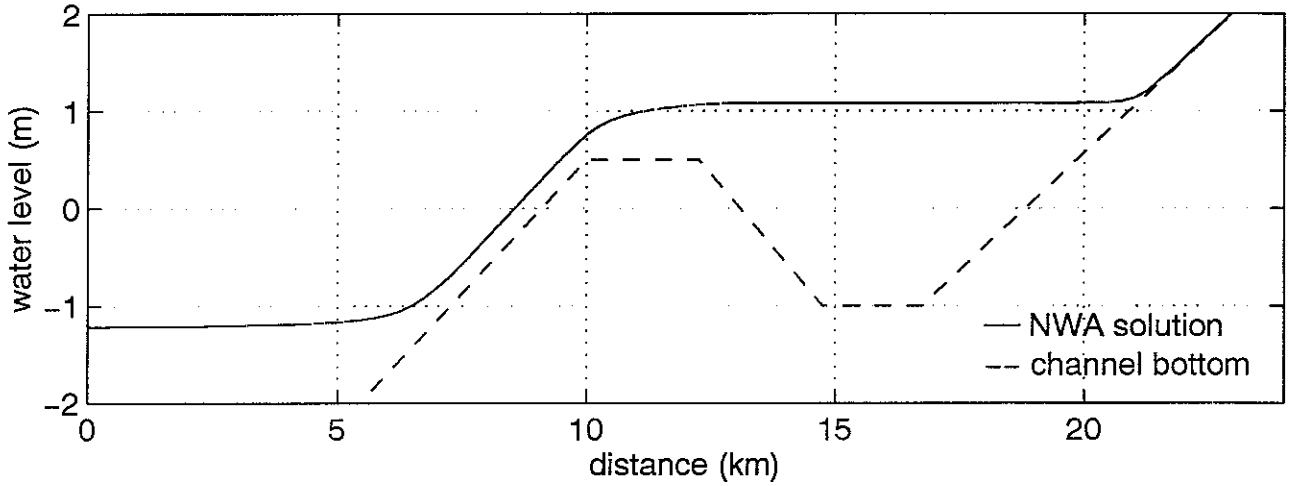

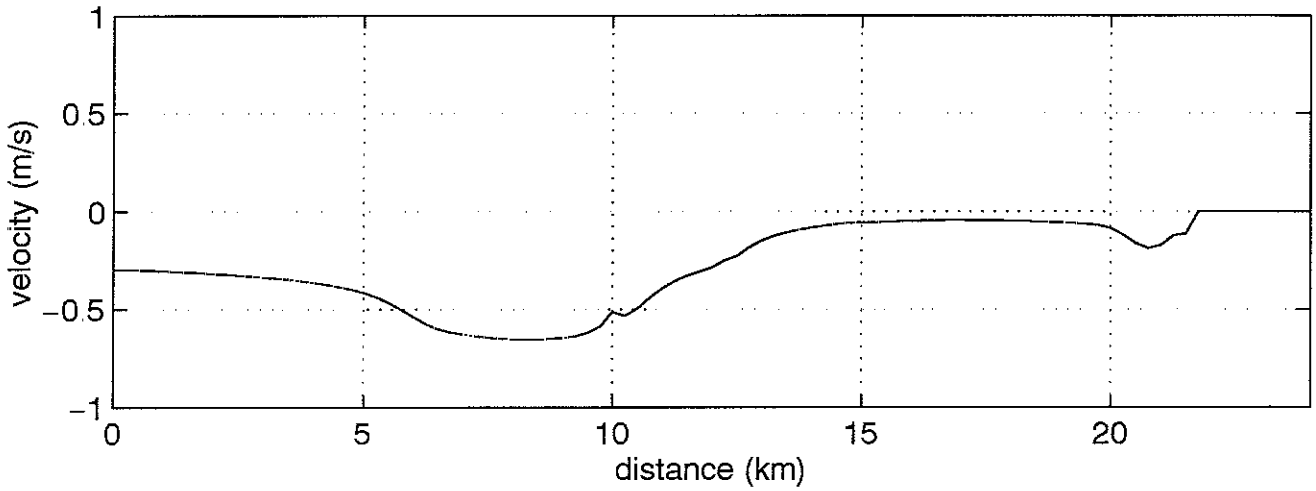

Figure 5f. Berm Test Case, Time = 5*T/10

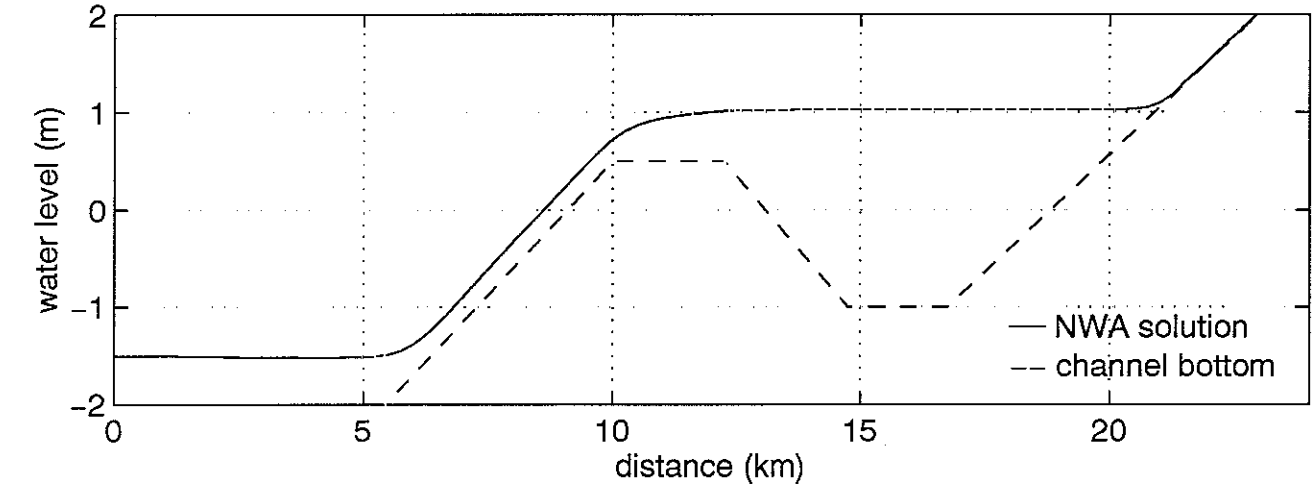

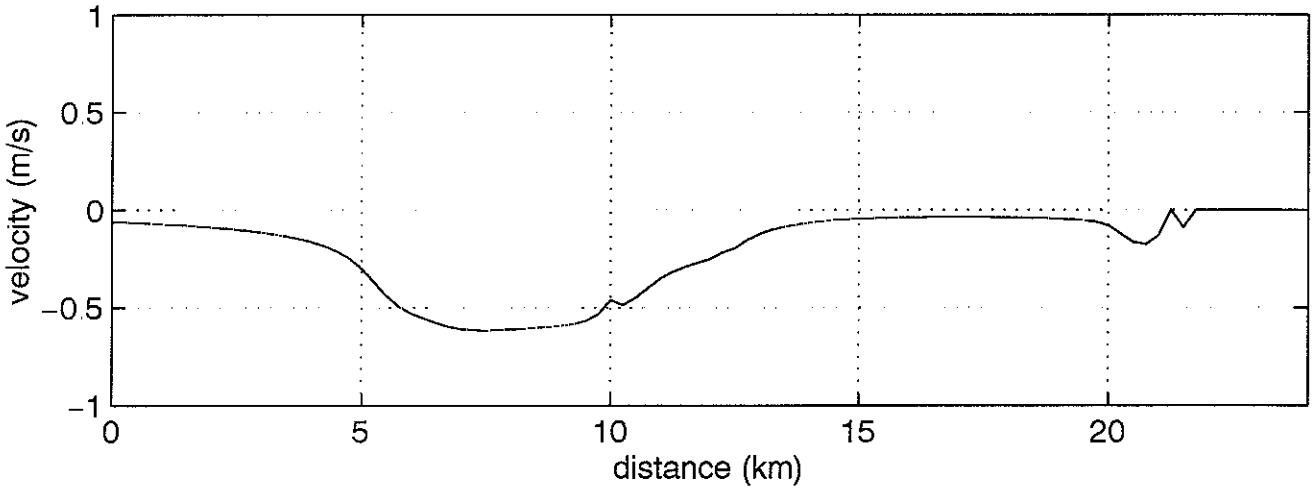

Figure 5g. Berm Test Case, Time = 6*T/10

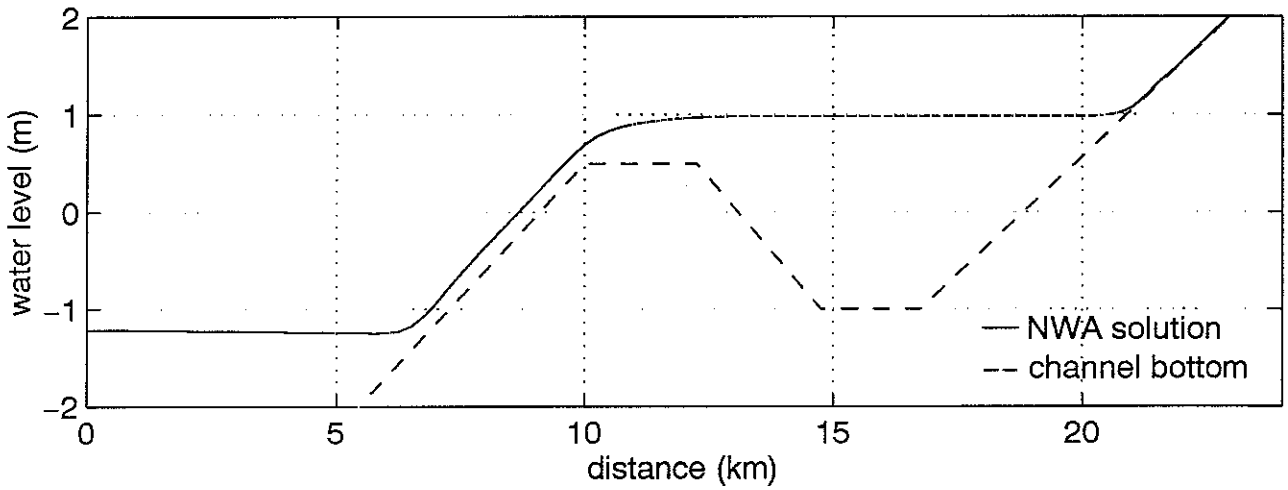

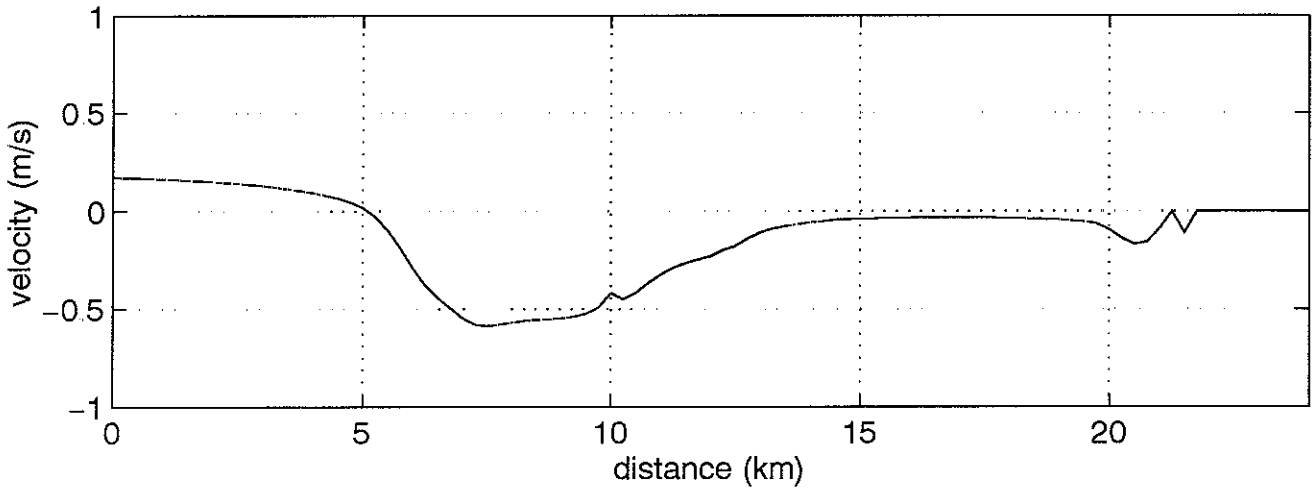

Figure 5h. Berm Test Case, Time = 7*T/10

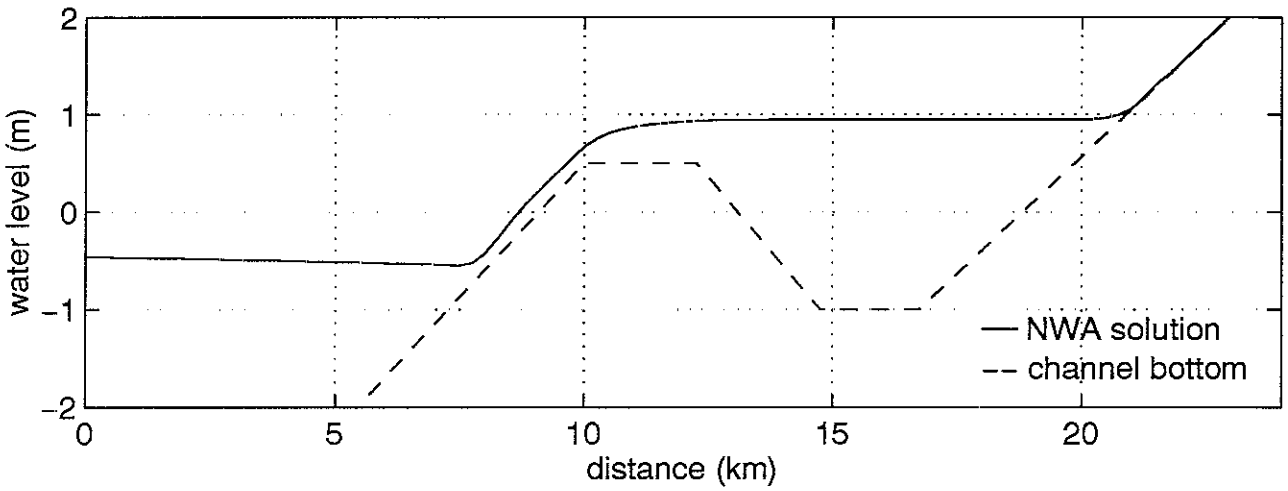

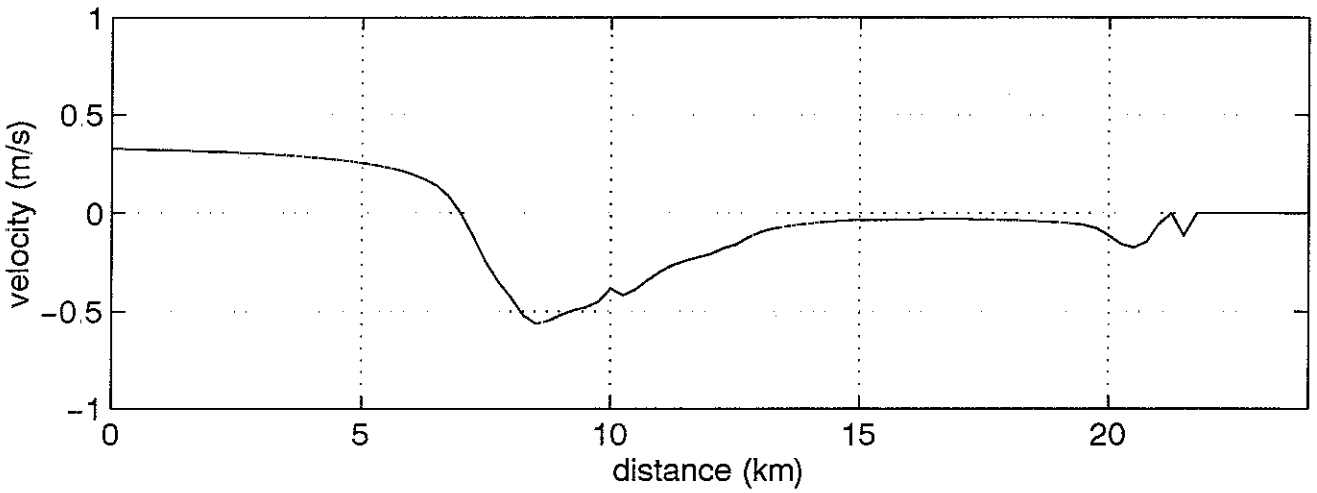

Figure 5i. Berm Test Case, Time = 8*T/10

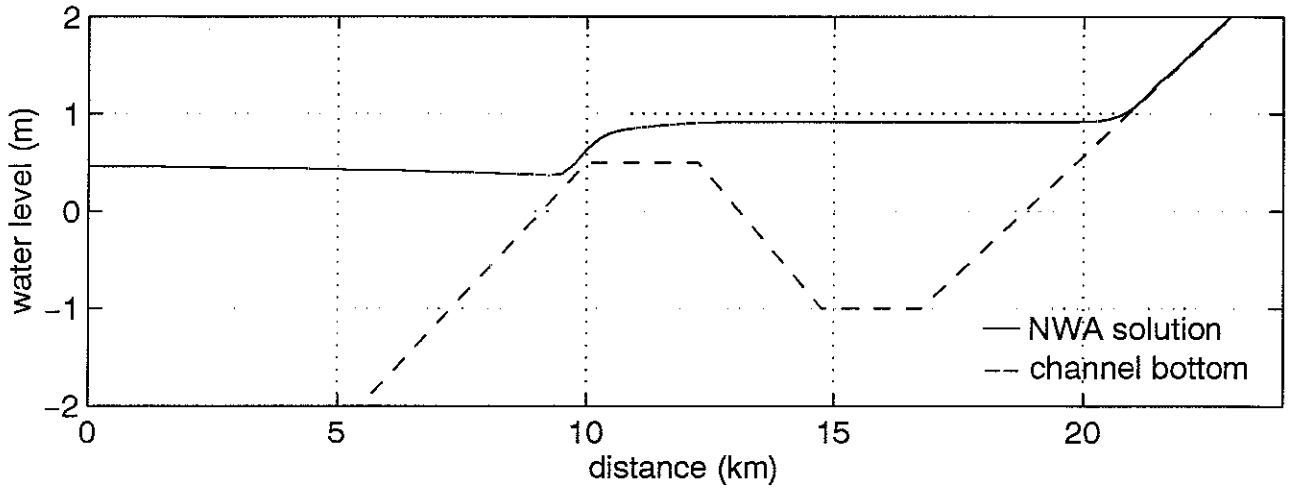

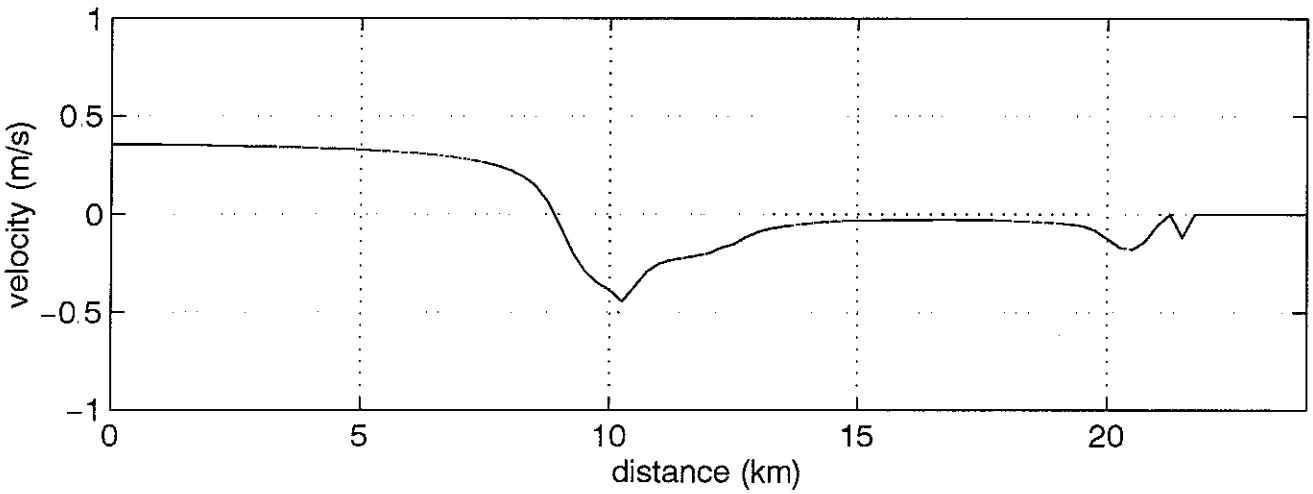

Figure 5j. Berm Test Case, Time = 9*T/10